



Introduction to Ultrafast Science and Technology

Chih-Wei Luo (羅志偉)

Department of Electrophysics,
National Chiao Tung University, Taiwan





Outline

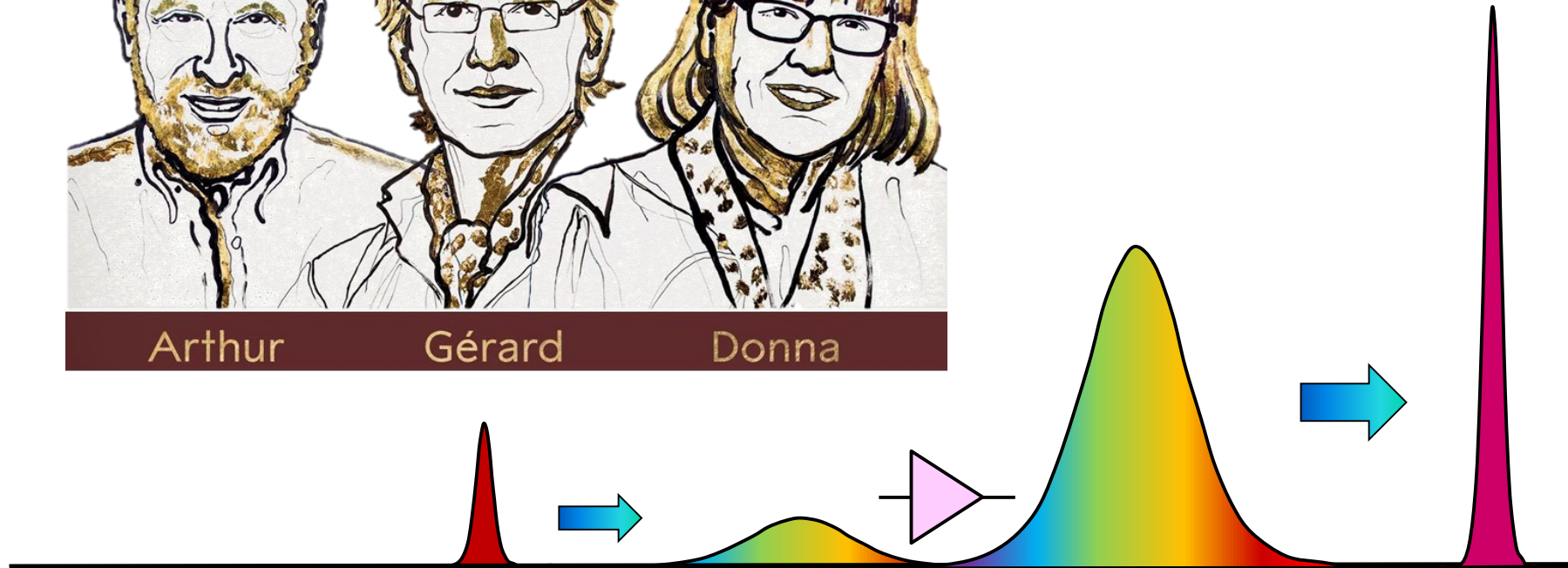
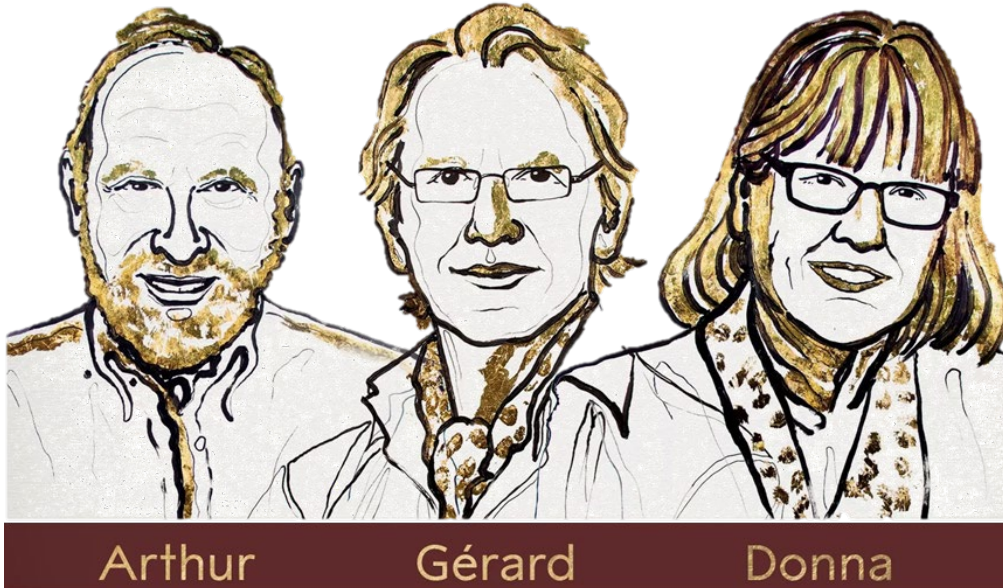
1. Introduction to femtosecond laser pulses
2. Nanoparticle fabrication
3. Nanostructure fabrication
4. Ultrafast dynamics in topological insulators





The Nobel Prize in Physics 2018

◆ Optical Tweezers & Chirped Pulse Amplification (CPA)





反其道而行的創新--啾頻脈衝放大

2018 諾貝爾物理獎 專輯

反其道而行的創新--啾頻脈衝放大

「在雷射物理領域的突破性發明」——這是2018年諾貝爾物理獎的得獎理由，由三位雷射科學的先驅共同獲得，這是繼1999年諾貝爾化學獎——將化學反應觀察尺度推進至飛秒級 (Femtosecond, 10^{-15} s) 和2005年諾貝爾物理學獎——利用超快雷射鎖模機制 (Mode-locking) 發展的雷射光梳 (Optical Frequency Comb) 之後，超快光學史上第三座諾貝爾獎，但不同於著重在時間尺度的飛秒化學反應及未知頻率量測的光梳技術，「啾頻脈衝放大」技術將脈衝雷射的尖峰功率提升至兆瓦 (Terawatt, 10^{12} W) 以上的等級。此項技術不但解決了雷射發展上的瓶頸——「在放大高強度雷射脈衝後，雷射脈衝會燒壞放大器」的棘手問題，並提供了可靠且精確的實現方法，使得高尖峰功率的脈衝雷射得以廣泛應用於各種領域，從雷射眼科角膜醫學手術、金屬和玻璃焊接到各類 3D 產品的製造中都可以見到它的足跡。

這項得獎工作於1985年在美国羅徹斯特大學 (University of Rochester) 的雷射能量學實驗室 (Laboratory for Laser Energetics, LLE) 完成。當時，Mourou 任教於羅徹斯特大學，Strickland 則是 Mourou 的博士生，並以「啾頻脈衝放大」為其研究主題，研究結果則刊登於光學通訊 (Optics Communications) 期刊上 [1]，這是她發表的第一篇論文。此外，Strickland 是第三位女性諾貝爾物理獎獲獎人。對此，美國物理聯合會 (American Institute of Physics, AIP) 表示「Strickland 打破了55年來沒有女性獲得諾貝爾物理學獎這一裂縫，使得今年的獎項更具有歷史意義。」 [2]

圖一：上圖是當前 (A) Mourou 與 (B) Strickland 的照片 (註：則則是當年 (C) Mourou 與 (D) Strickland 在羅徹斯特大學的照片)。

對此，羅徹斯特大學光學研究所所長——Scott Carney 形容 [5]「這對光學領域來說是一個偉大的日子，而且毫無疑問地在光學上的衝擊早已橫跨科學及工程兩大領域。啾頻脈衝放大技術打開了通往科學寶庫的大門。如果沒有這種令人難以置信的強大而精美的發明，我們仍然會生活在奈秒 (Nanosecond, 10^{-9} s) 級的世界中，而無法探索速度快一百萬倍的飛秒動力學物理。從化學到大氣科學；從非線性量子電動力學到雷射加工製造都可看到 Mourou 教授和 Strickland 教授的工作所造成的重大影響。這種認可絕對是當之無愧的。」確實，從38頁的圖一可以看出，當「啾頻脈衝放大」技術在1985年被發明之後，脈衝雷射的尖峰功率進入了另一個檔次。目前，這項技術已成為市售脈衝雷射放大器的標準架構，也為學術研究及工業應用帶來無限的可能。

甚麼是「啾頻脈衝放大」?

首先，讓我們介紹何謂「脈衝」：如圖二所示，當只有單一頻率 (顏色) 的光波存在於雷射時，雷射輸出光為「連續波」的形式，也就是雷射光強度隨時間變化維持一定值，不會改變。但當有數個頻率 (顏色) 的光波同時存在於雷射中且相互之間的相位維持不變，則會因為干涉效應造成輸出光為「脈衝波」的形式，也就是雷射光強度隨時間增加變大又變小，只有在某一時間點才有雷射光，其他時間則無雷射光的存在。此外，如果這些可以互相疊加及干涉的雷射光頻率 (顏色) 越多，即頻寬越寬，就可以在時間軸上疊加並干涉成越窄的脈衝，同時脈衝強度也會增加。以上結果可用我們熟悉的傅立葉轉換原理來說明。如果我們可以不斷增加頻域 (Frequency domain) 中的頻寬 (Bandwidth)，也就是可以互相干涉的雷射光頻率 (顏色) 數量越多，則可以在時域 (Time domain) 中製造出脈衝寬度 (Pulse width) 更窄、強度更強的超短脈衝 (Ultrashort pulse)。

模態 (mode)	頻寬 (Bandwidth)	脈衝寬 (Pulse width)	
A 單一波長	趨近於0	趨近於無窮	連續波
B 頻寬較窄		長脈衝	
C 頻寬較寬 (無色散)		超短脈衝	
D 頻寬較寬 (有色散)		啾頻脈衝	

圖二：脈衝寬與其頻寬之間的關係



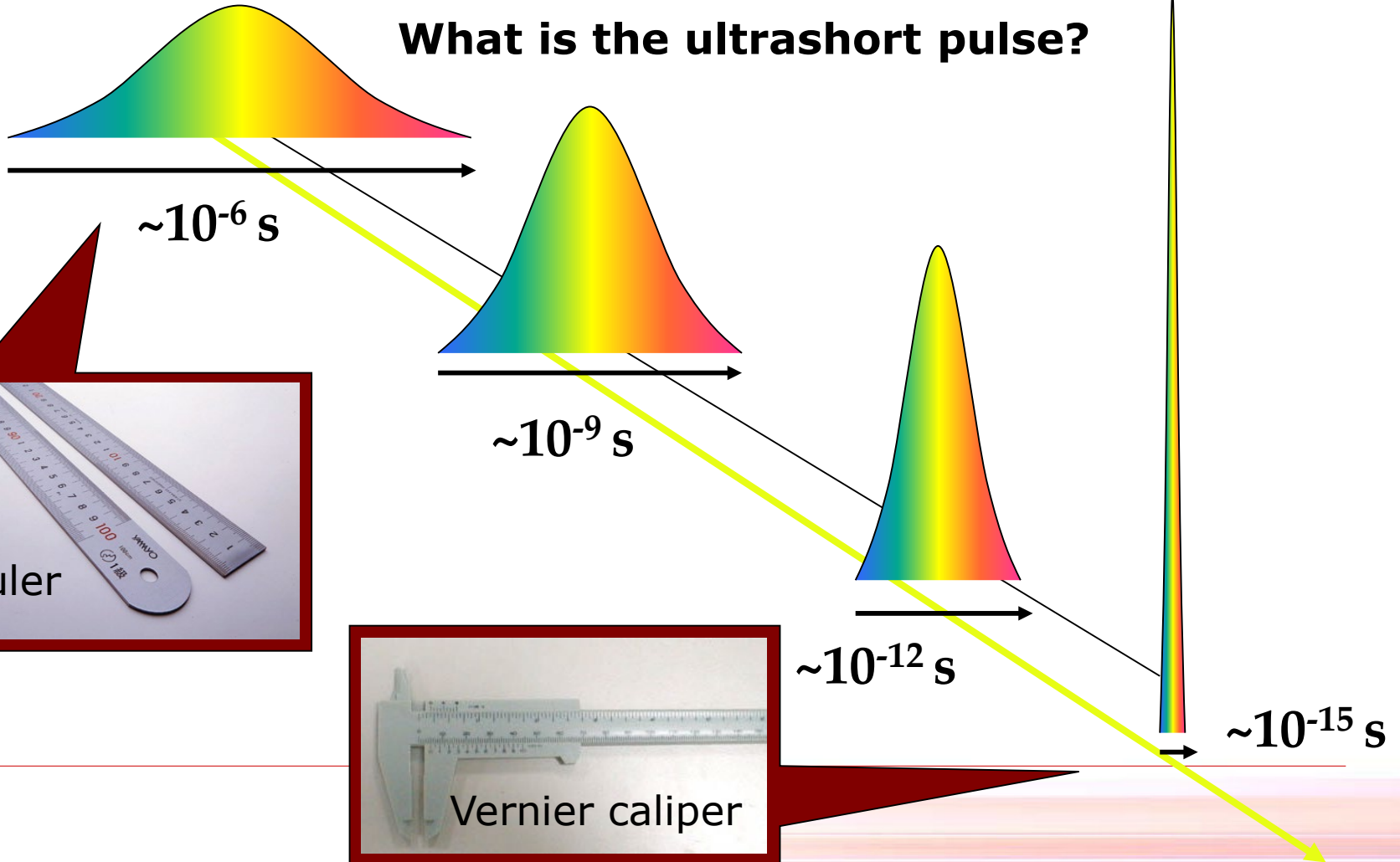
羅志偉、葉恬恬

物理雙月刊 2月號/2019 41卷第1期



Introduction to fs laser pulses

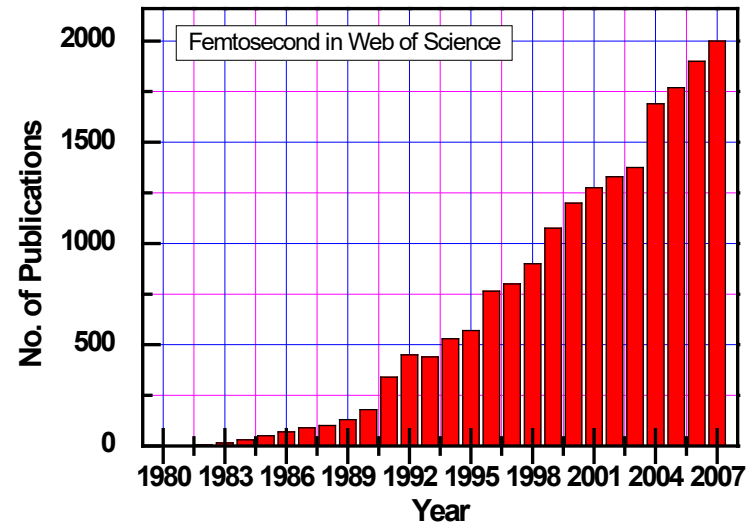
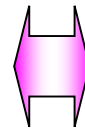
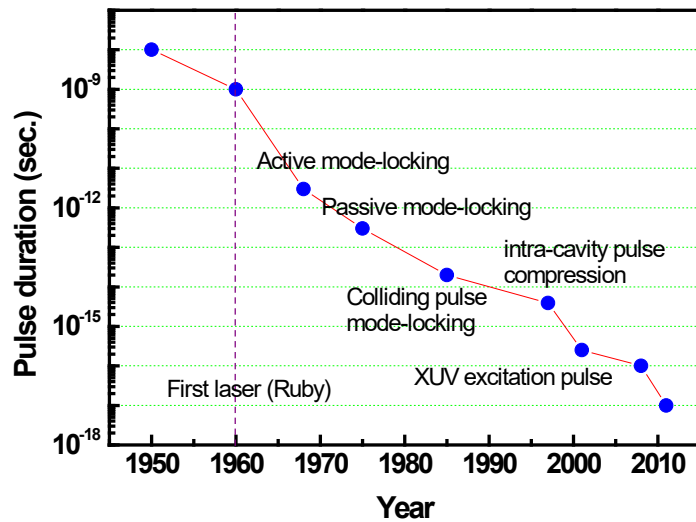
What is the ultrashort pulse?





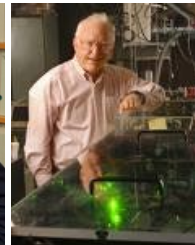
Introduction to fs laser pulses

The shorter pulse duration, the more papers!



Prof. Ahmed Zewail

The 1999 Nobel Prize in Chemistry



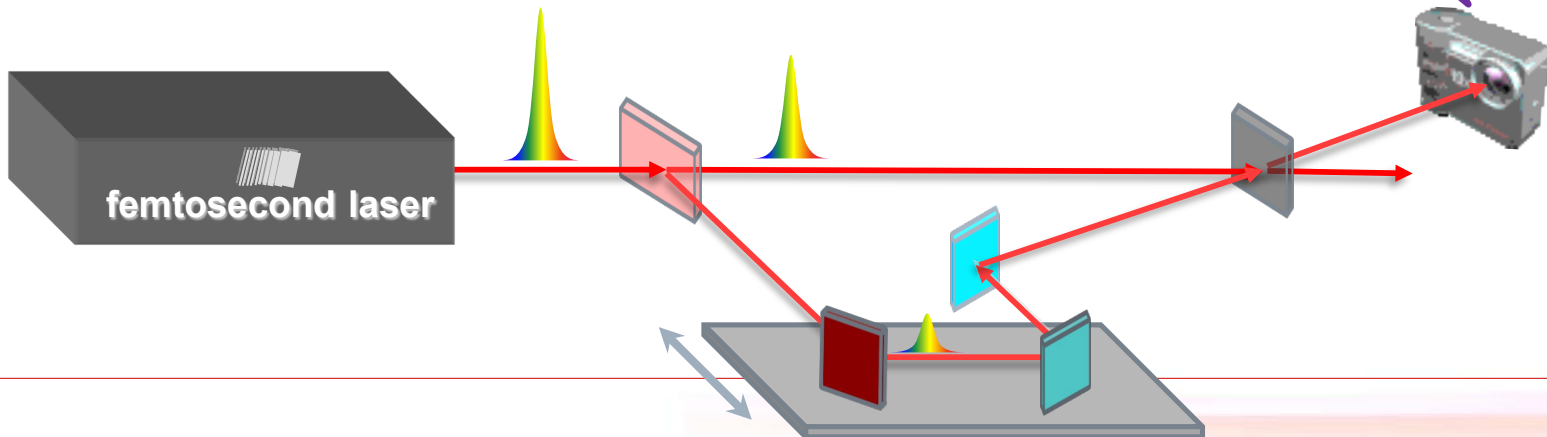
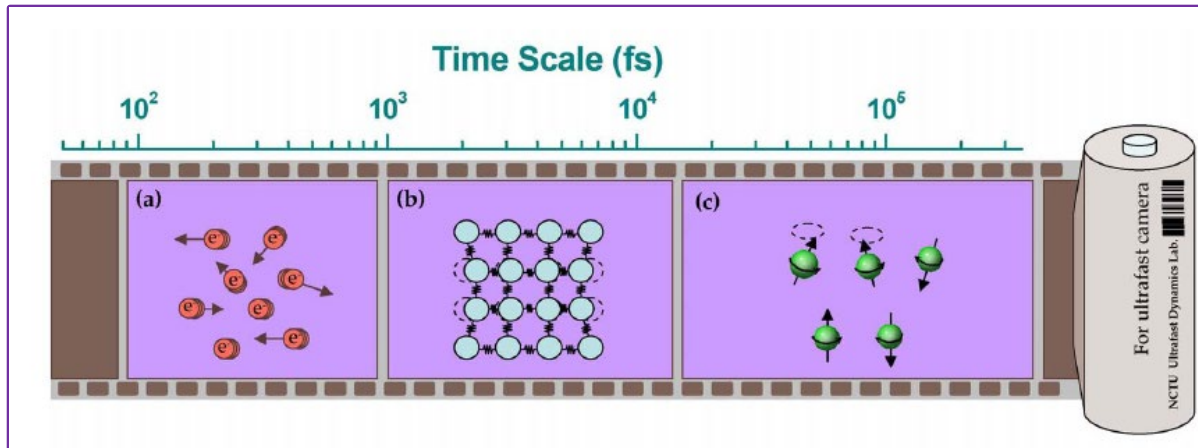
Prof. Theodor W. Hänsch & Prof. John L. Hall

The 2005 Nobel Prize in Physics



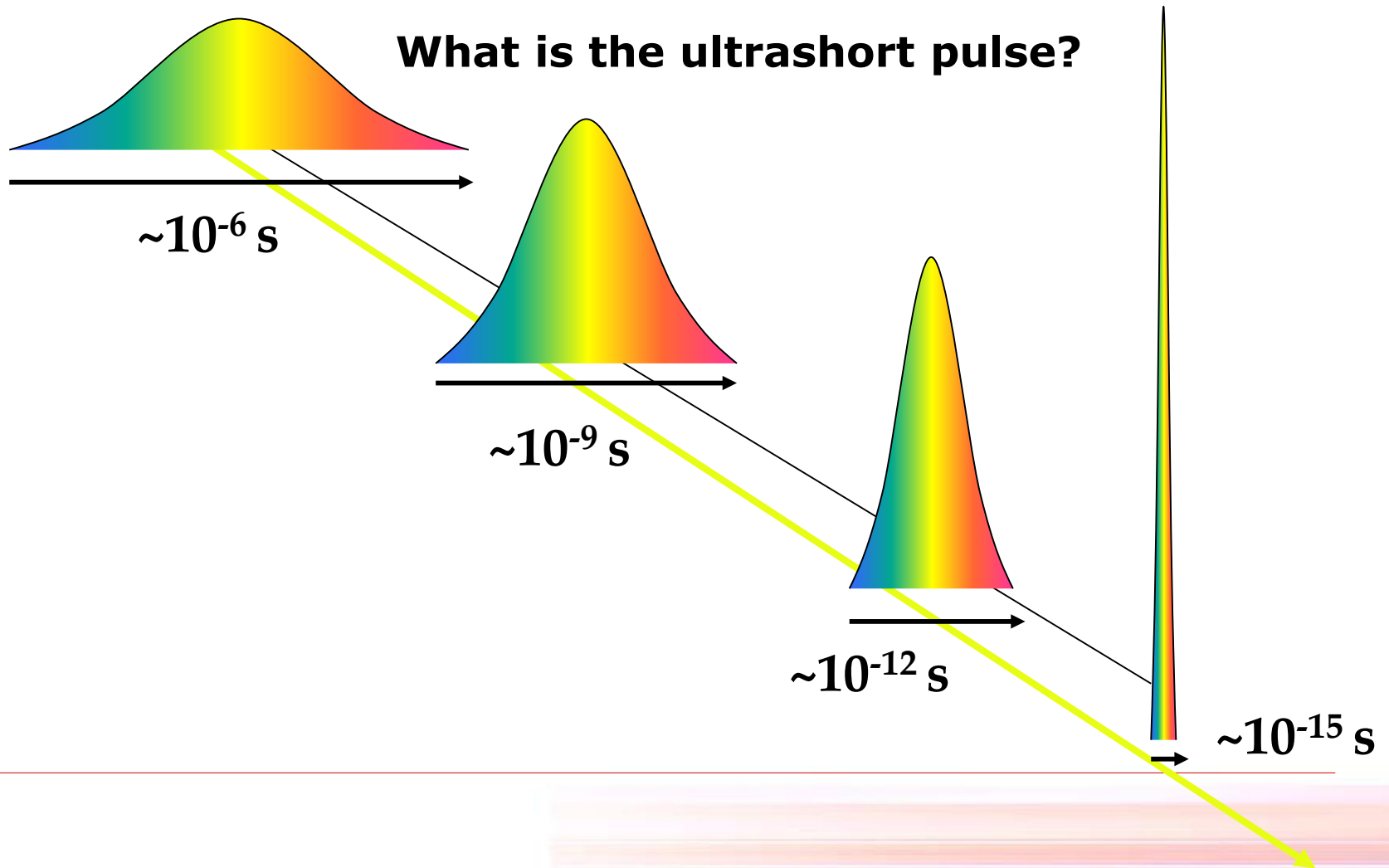
Introduction to fs laser pulses

Ultrafast camera!!





Introduction to fs laser pulses





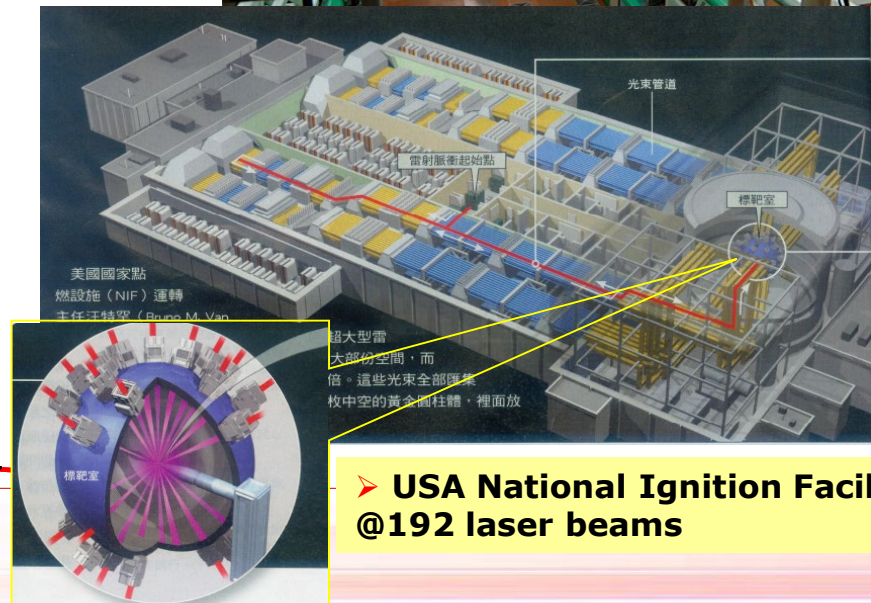
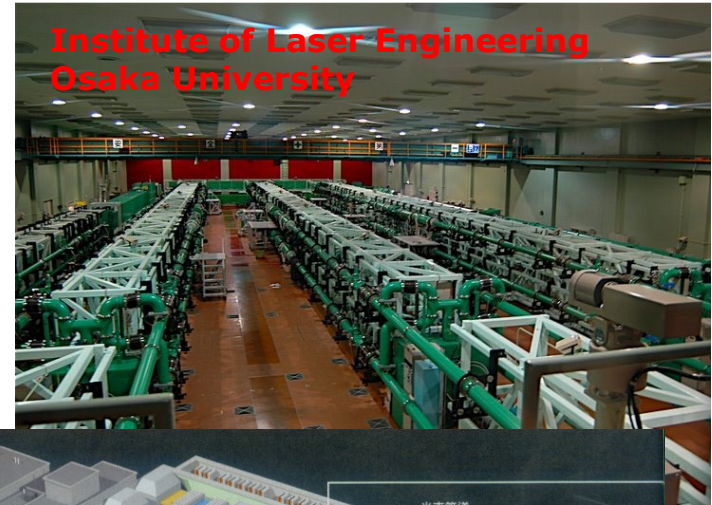
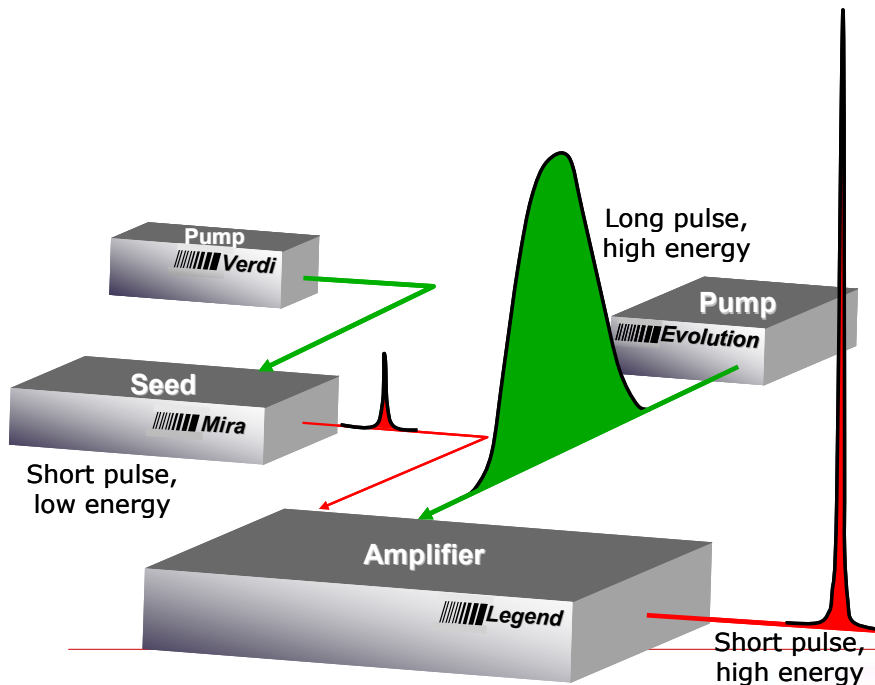
Introduction to fs laser pulses

The possibility for nuclear fusion!

Short pulse = intense peak power

→ 100 mJ, 100 fs = 1 TW

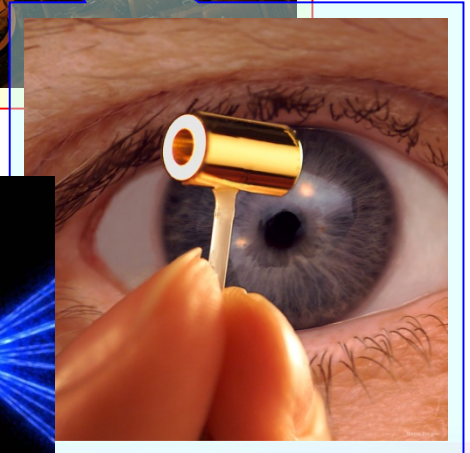
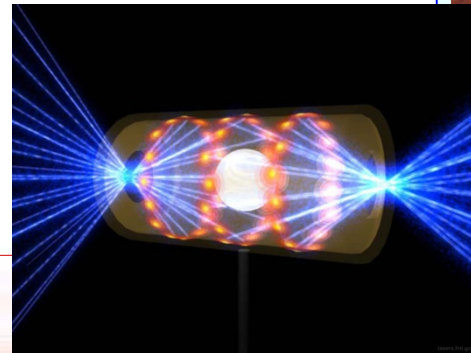
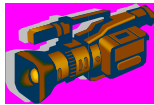
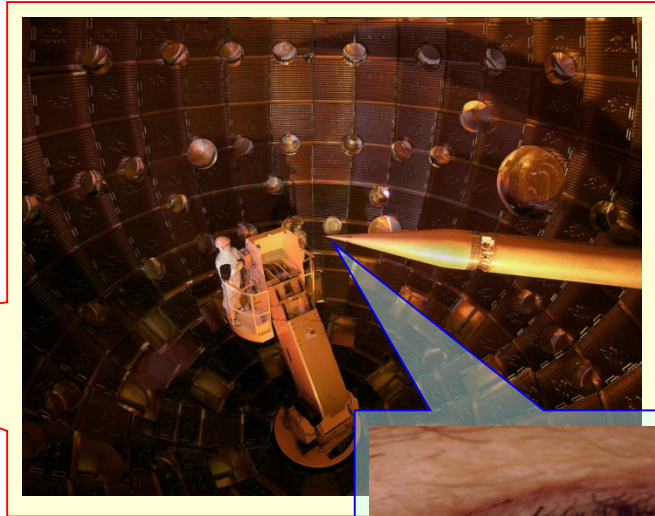
→ 10^{18} W/cm² @ $\phi = 10 \mu\text{m}$ (10^{10} V/cm)





Introduction to fs laser pulses

USA National Ignition Facility



➤ Output power ~ 300 TW



美首次實證雷射核融合 放出超量能量

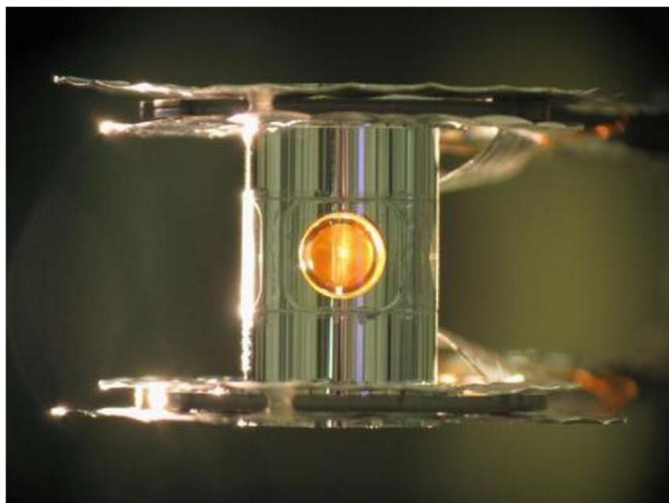
作者: NewTalk 新頭殼 | 新頭殼 - 2014年2月13日 上午9:18

新頭殼newtalk 2014.02.13 鄭凱榕/編譯報導

美國能源部所屬國家研究機構「勞倫斯利福摩爾國家實驗室」(Lawrence Livermore National Laboratory, LLNL)的研究團隊首次確認,使用高功率雷射進行核融合實驗,從燃料所釋放出來的能量,超出投入的能量。這項研究結果12日發表在英國科學期刊《自然》電子版。

根據日本共同通信社13日華盛頓報導,研究團隊利用在太陽星體上發生的相同現象,證明了從非常少的燃料可以釋放出很大的能量,未來將有可能使用核融合發電。但是在這項技術如果要應用,還有非常多的技術課題有待克服。研究團隊的負責人表示,「終於來到了為了登山攻頂所需的基地營」。

核融合,是指在超高溫、高壓下,輕原子核融合轉變成重原子核的現象。根據維基百科的說明,核融合將諸如氫原子核一類的較輕的原子核結合形成較重的原子核。



LETTER

doi:10.1038/nature13008

字 + 字

Fuel gain exceeding unity in an inertially confined fusion implosion

O. A. Hurricane¹, D. A. Callahan², D. T. Casey², P. M. Collier³, C. Cerjan⁴, E. L. Dewald¹, T. R. Dittrich², T. Döppner⁵, D. E. Hinkel⁶, I. F. Berzak Hopkins⁶, J. L. Kline⁷, S. LePape⁸, T. Ma⁹, A. G. MacPherson¹⁰, I. L. Mitsuhashi¹¹, A. Pak¹², H.-S. Park¹³, P. K. Patel¹⁴, R. A. Remington¹⁵, I. D. Salmonson¹⁶, P. T. Springer¹⁷ & R. Tommasini¹⁸

Ignition is needed to make fusion energy a viable alternative energy source, but has yet to be achieved¹. A key step on the way to ignition is to have the energy generated through fusion reactions in an inertially confined fusion plasma exceed the amount of energy deposited into the deuterium-tritium fusion fuel and hot spot during the implosion process, resulting in a fuel gain greater than unity. Here we report the achievement of fusion fuel gains exceeding unity on the US National Ignition Facility using a 'high-foot' implosion method²⁴, which is a manipulation of the laser pulse shape in a way that reduces instability in the implosion. These experiments show an order-of-magnitude improvement in yield performance over past deuterium-tritium implosion experiments. We also see a significant contribution to the yield from α -particle self-heating and evidence for the 'bootstraping' required to accelerate the deuterium-tritium fusion burn to eventually 'run away' and ignite.

At the National Ignition Facility (NIF), 192 laser deliver up to 1.9 MJ of light into a gold hohlraum, a cylindrical-shaped radiation cavity (Fig. 1), that converts the energy into a nearly Planckian X-ray bath. A fraction of the X-rays are absorbed by a capsule generating ~ 100 Mbar of pressure in the ablator (the outer shell of the capsule). This ablation pressure, delivered as a series of weak shocks, accelerates the capsule inward. Against the inside of the ablator is the deuterium-tritium (D-T) fuel shell, which is initially in a cryogenic state. When

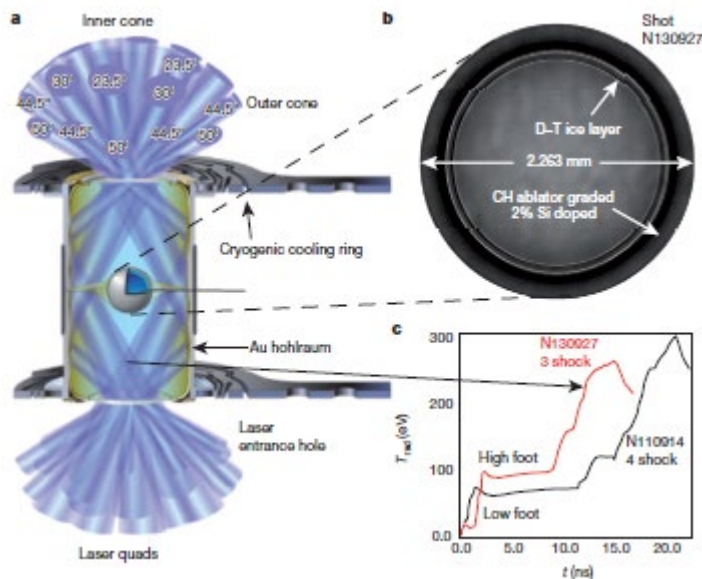
The high-foot implosion is designed to reduce ablation-front-driven instability growth and thereby inhibit ablator plastic (carbon-hydrogen and silicon dopants) from mixing into and contaminating the D-T hot spot. The laser pulse shape is designed to obtain a relatively high hohlraum radiation temperature ($T_{\text{rad}} \sim 90$ –100 eV) during the foot of the pulse (Fig. 1) and launch a three-shock. In contrast, the NIF implosion pulse shape drives a lower radiation temperature ($T_{\text{rad}} \sim 60$ eV) in the foot (hence 'low-foot') for longer and launch four shocks. The essential stability benefits of the high-foot growth can be understood from examining an expression for the linear growth rate of the ablation-driven Rayleigh-Taylor instability²⁵

$$\gamma_{\text{RT}} \approx \alpha(F_r, v) \sqrt{\frac{kg}{1 + R_p}} - \beta(F_r, v)kv, \quad (1)$$

where k is the perturbation wavenumber, g is the ablator acceleration, L_p is the density gradient scale length of the ablation front, v is the ablation velocity, and α and β are parameters of order unity whose exact values depend on a host of conduction scale-length parameters, χ and the Froude number, $Fr = v^2/(g L_p)$. The key stabilizing effects of the high-foot drive enter through higher ablation velocity, which scales as $T_{\text{rad}}^{1/2}$, increasing the βkv , which has a stabilizing term of equation (1), and through an increase in L_p , which reduces the instability term proportional to \sqrt{kg} . The increase in L_p is primarily due to a stronger first shock, which is absent in the implosion and prevents the ablator from being highly compressed (raking break-up) during the implosion. Instability can be further understood by comparing the light aspect ratio ($R_{\text{light}}/\Delta R$), where R_{light} is the ablator inner to the ablator thickness) of the high- and low-foot implosions. In the high-foot implosion, the light aspect ratio is roughly low-foot implosion—the amplitude of instability growth is reduced to the exponential of $\sqrt{R_{\text{light}}/\Delta R}/2$ (ref. 11). The trade-off between the improved stability of the high-foot implosion is fuel adiabat, $\alpha = P/\rho$ (usually denoted as β), where P is the Fermi pressure, is higher, making the fuel less compressible for a given amount of ablation energy. (An alternate to ablat using P_{min} the minimum D-T pressure at ionization onset²⁴). Details of the stability benefits, other trade-offs and trade-offs involved in the high-foot implosion results from the first set of five D-T implosion is described elsewhere²⁴.

deuterium-tritium implosions N130927 and N131119 (NIF shot on-month-day format YYMMDD) build on the previous (N130812²⁴), by modestly increasing the NIF laser power (table 1) and by redistributing energy between different rough laser wavelength channels that affect the cross-section of power from one beam to another via scattering, to optimize the illumination pattern in

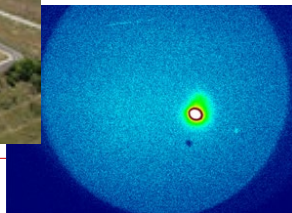
© 2014 Nature Publishing Group





Introduction to fs laser pulses

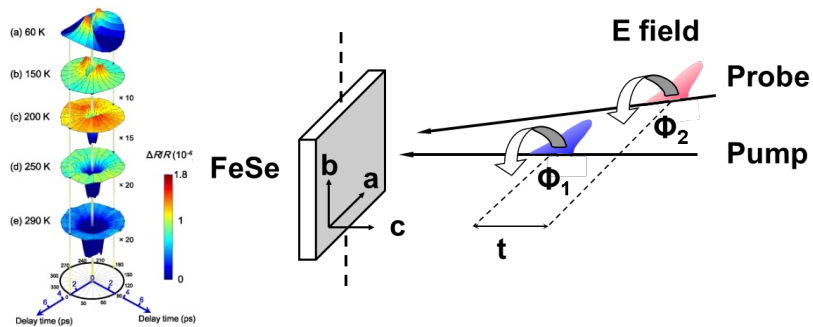
Free electron laser - Japan



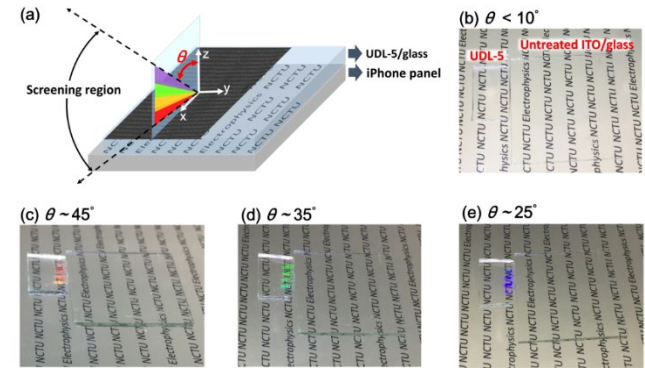


Researches in Ultrafast Dynamics Lab

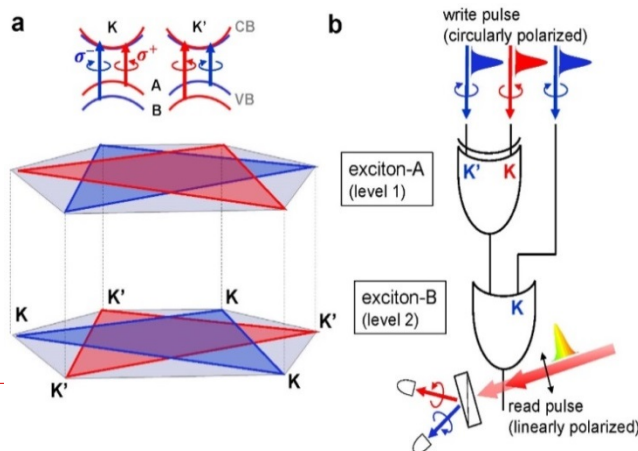
Superconductors



Femtosecond laser annealing



2D materials – Graphene, MoS₂



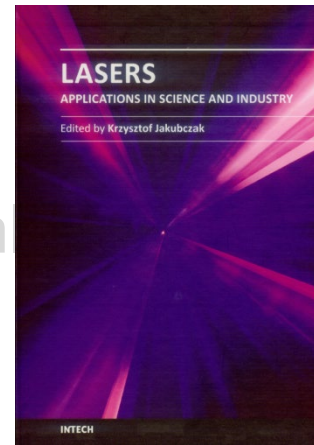
Selected publications

- 1) **Adv. Optical Mater.** 1, 804-808 (2013)
- 2) **Nano Lett.** 13, 5797 (2013)
- 3) **Nanoscale** 6, 8575 (2014)
- 4) **Nano Energy** 15, 625 (2015)
- 5) **Advanced Materials** 28, 876 (2016)
- 6) **Advanced Functional Materials** 26,729 (2016)
- 7) **Optica** 3, 82 (2016)
- 8) **npj Quantum Materials**, 2, 1 (2017)
- 9) **Optics Express** 25, 33134 (2017)
- 10) **Nano Lett.** 18, 7742 (2018)
- 11) **Phys. Rev. Materials** 3, 034802 (2019)
- 12) **Optics Express** 28, 685 (2020)



Outline

1. Introduction to femtosecond laser pulses
2. Nanoparticle fabrication
3. Nanostructure fabrication
4. Ultrafast dynamics in topological



1
Nanoparticles and Nanostructures Fabricated Using Femtosecond Laser Pulses
 Chih Wei Luo
 Department of Electrophysics, National Chiao Tung University, Taiwan
 Republic of China

Lasers – Applications in Science and Industry
Nanoparticles
 Since the 1970s for implementation in electrical and optical properties of doped polymers [Ding et al., 2000; Xiang et al., 2009], Abjigit has had a tremendous impact on structures of ZnSe, in particular, have been fabricated using femtosecond laser pulses, cubic and hexagonal. In addition, ZnSe has been used for the hexagonal structure in ZnSe [Che et al., 2004]. In this section, we discuss the fabrication of ZnSe nanoparticles using femtosecond laser pulses.

ing of materials by femtosecond (fs) laser pulses has attracted a great deal of interest since the 1990s. In particular, periodic structures can be precisely and rapidly transferred to the substrate by using fs laser pulses. In particular, periodic structures can be produced in almost any materials using fs pulses directly and without the need for chemical photoresists to relieve the environmental concerns [Hsu et al., 2007; Luo et al., 2008; Sakai et al., 2009; Jin et al., 2010; Liu et al., 2010; Kim et al., 2010; Okamoto et al., 2010; Huang et al., 2009; Luo et al., 2008; Teng et al., 2010; Anagnostou et al., 2010]. (Zhou et al., 2007) have been induced in various materials using fs laser pulses. In addition, fs laser ablation for metals and dielectrics in vacuum environment [Anagnostou et al., 2004; Liu et al., 2007a] and in air [Luo et al., 2007b] have also been extensively investigated. These results are a strong indication of the potential of fs laser pulses in science and industry.

demonstrate the generation of nanoparticles and nanostructures (dots) using fs laser pulses. Initially, we selected the D-VT to demonstrate the fabrication of nanoparticles. Following the pulses at a wavelength of 800 nm and pulse duration of 80 fs, many nanoparticles formed on the surface of an undoped (UD) cubic ZnSe. The interesting phase transition from the cubic structure of ZnSe to single-crystal structure of ZnSe nanoparticles may have been caused by the laser pulse at the local area due to the sudden appearance of high-energy transition. This chapter discusses the details of the mechanism underlying this process.

In the second part of this chapter, we introduce controllable nanoparticle and nanodot structures to high-T_c superconducting YBaCuO (YBCO) thin films. We also introduce the surface morphology of YBCO thin films under single-beam and dual-beam fs laser irradiation. The generation of periodic ripple and dot structures is determined by the application of laser fluence, the number of pulses, polarization and the incident angle of the laser beam. The period and orientation of ripples and even the size and density of dots can be controlled by these parameters.

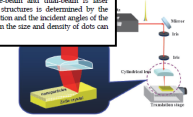


Fig. 1. Experimental setup for the fabrication of ZnSe nanoparticles.





**“Can we utilize the femtosecond pulses
to obtain ZnSe nanoparticles?”**

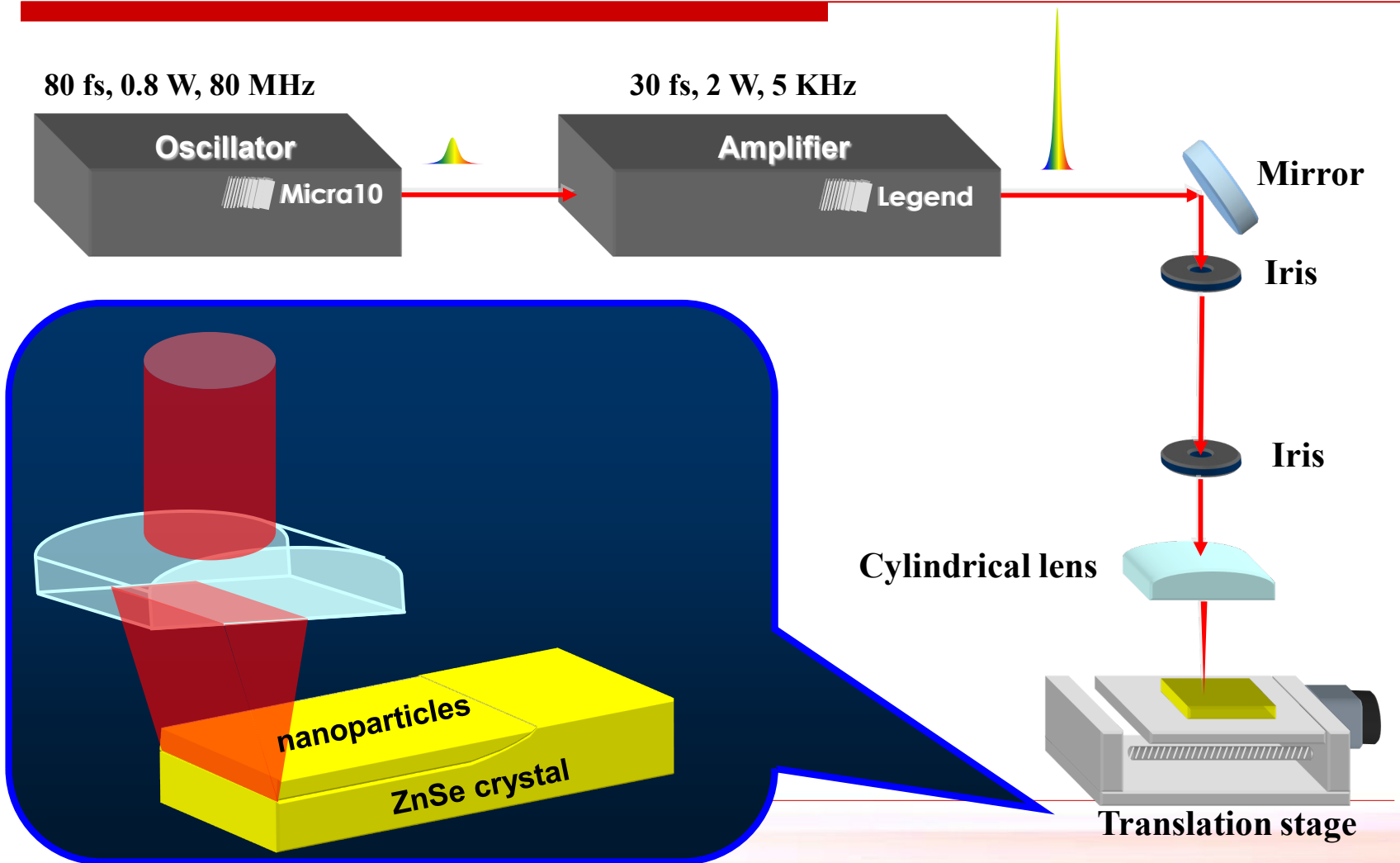
Simple!

Pure!

Fast!

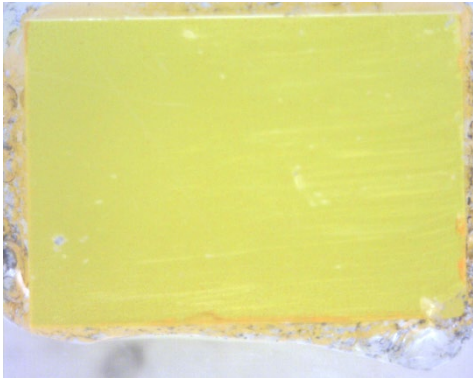


Experimental setup

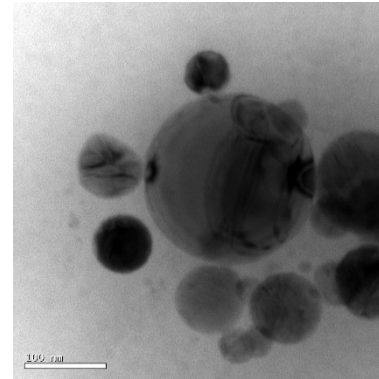




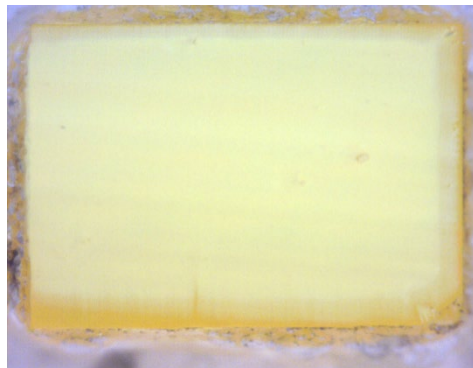
Experimental procedure



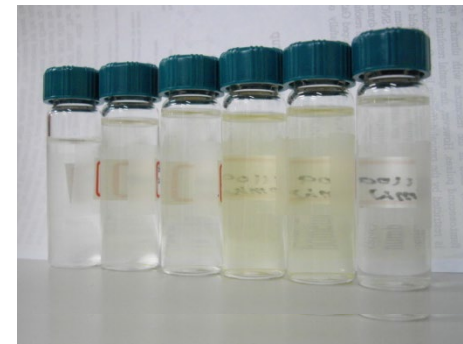
Before laser process



TEM image measurement



After laser process

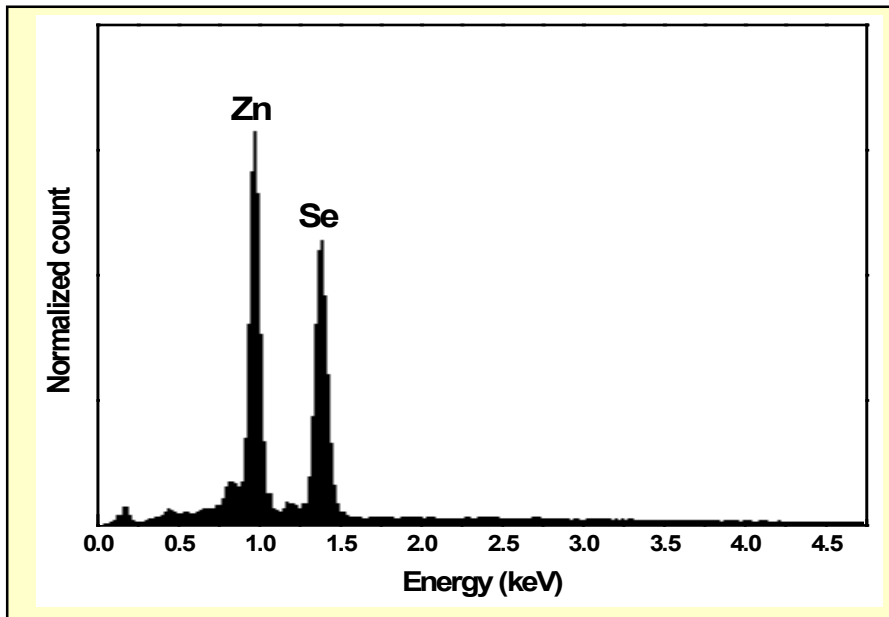


Dispersion in ethanol

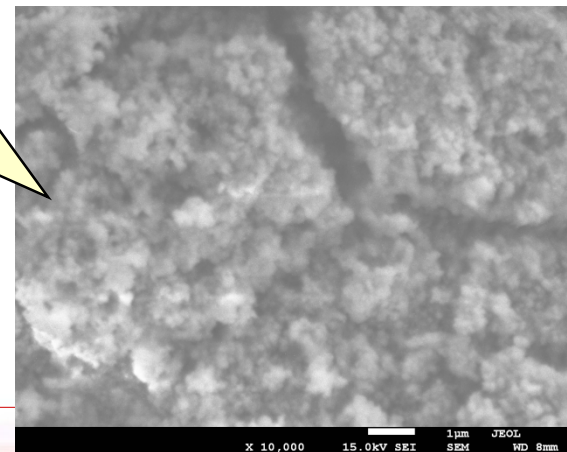


Composition of ZnSe nanoparticles

The EDX spectrum



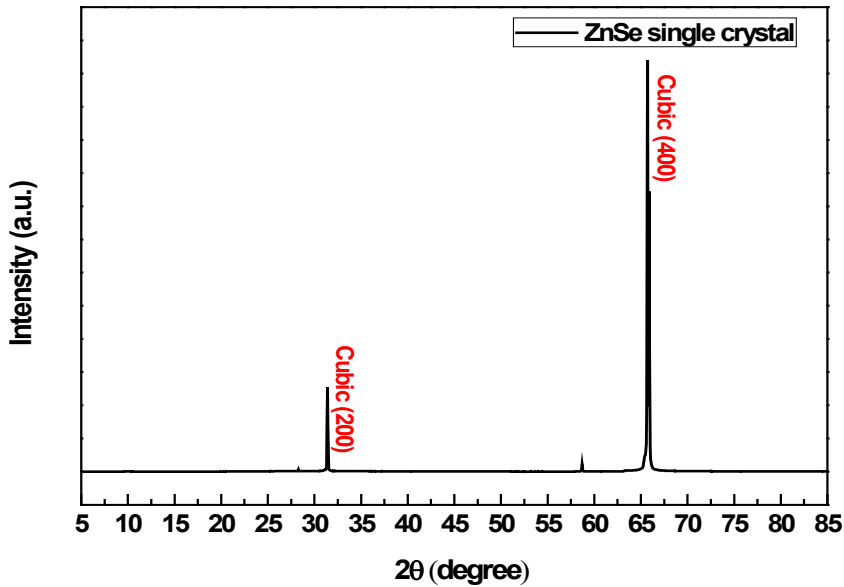
- The main elements in nanoparticles are **zinc** and **selenium**.
- The molar ratio of Zn and Se \sim **1 : 1**.



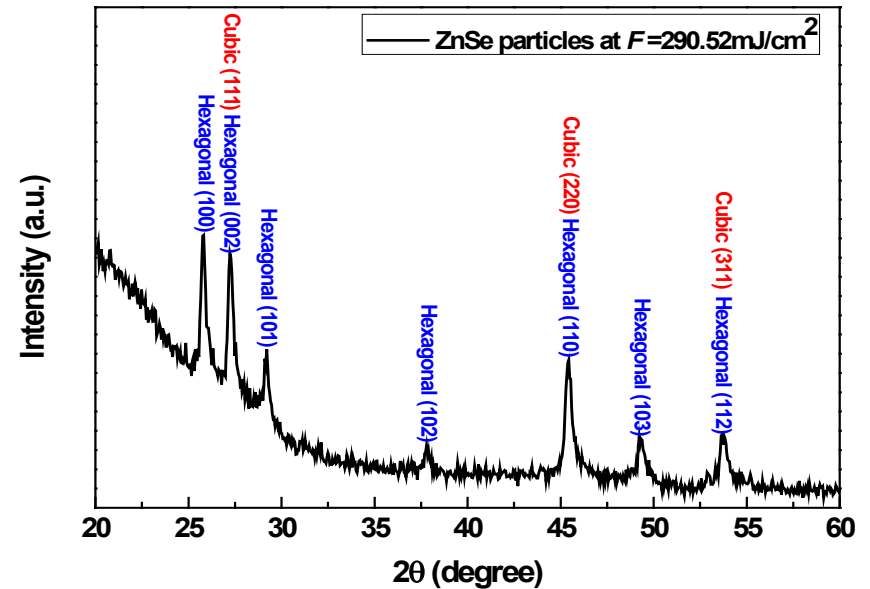


Structural phase transition

XRD results



Cubic structure
ZnSe single crystal

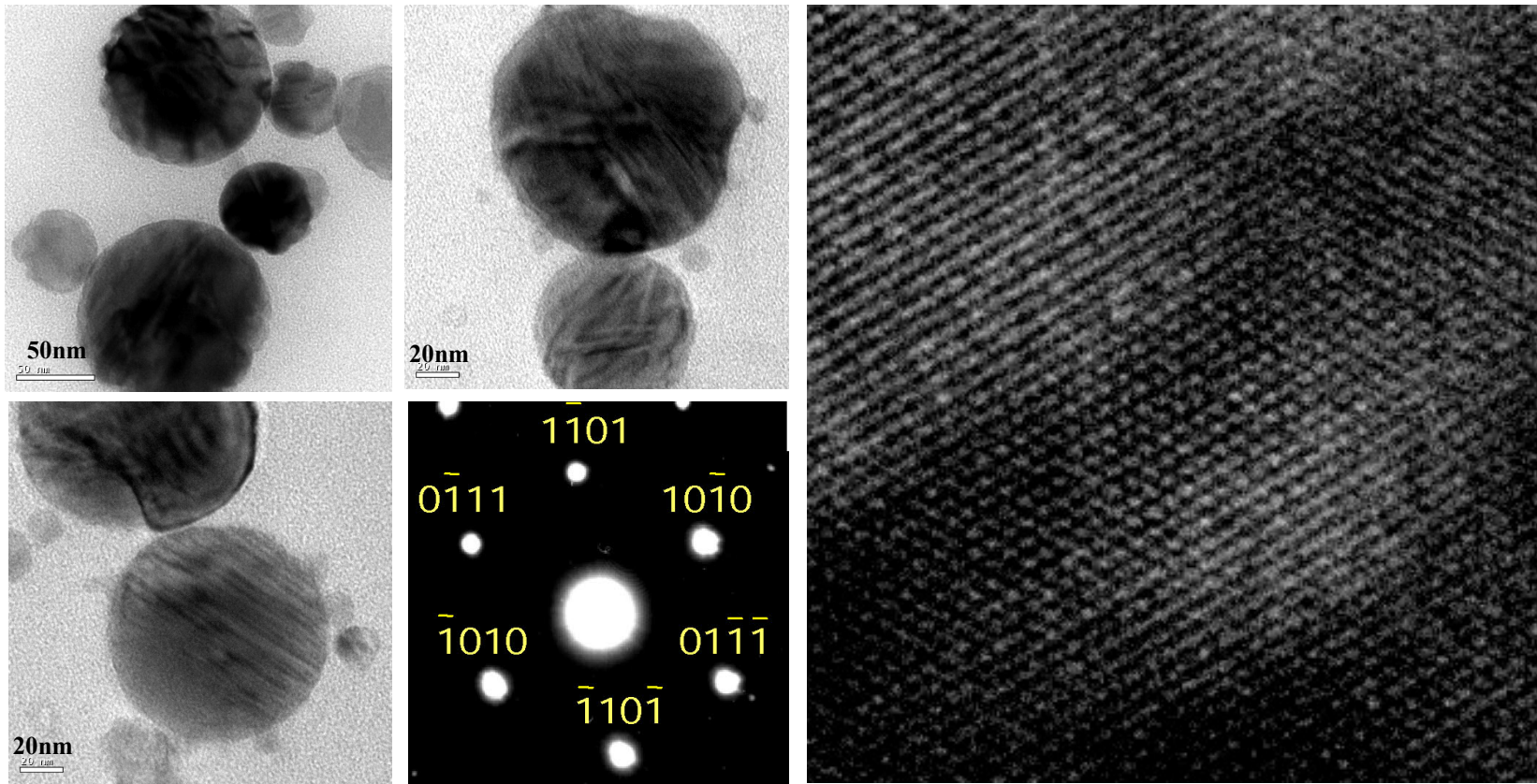


Hexagonal structure
ZnSe nanoparticles

Femtosecond laser process



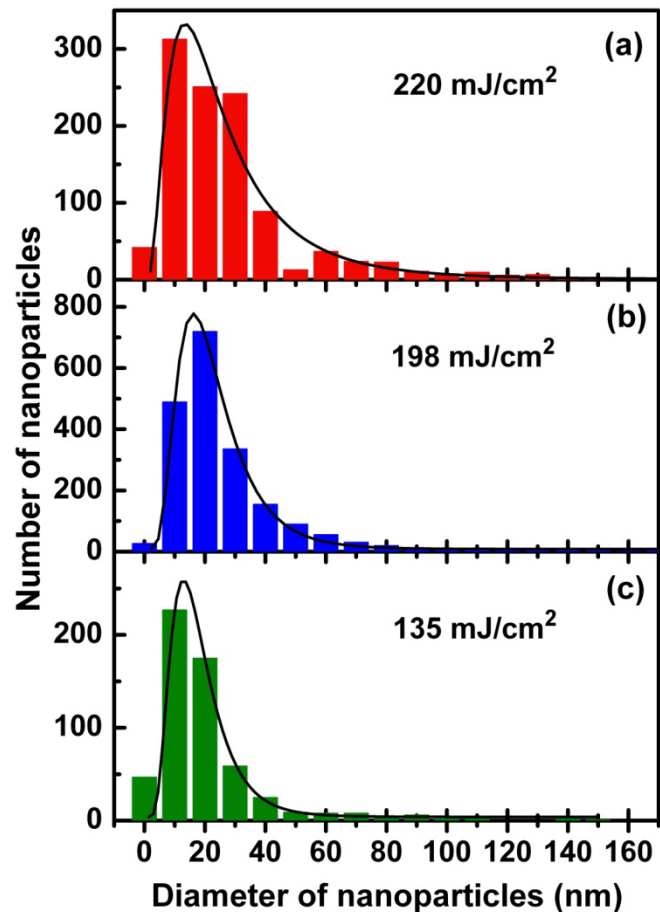
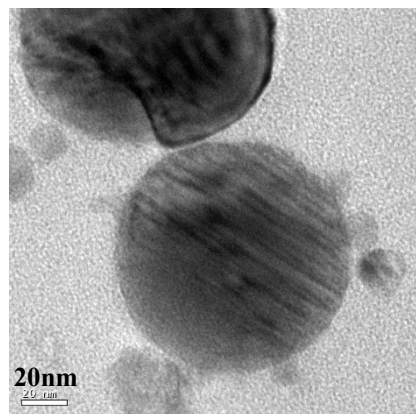
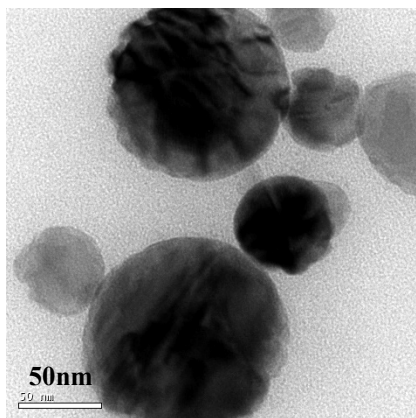
TEM image of ZnSe nanoparticles



The size of ZnSe particles are **< 100 nm** for laser fluence = 127 mJ/cm²

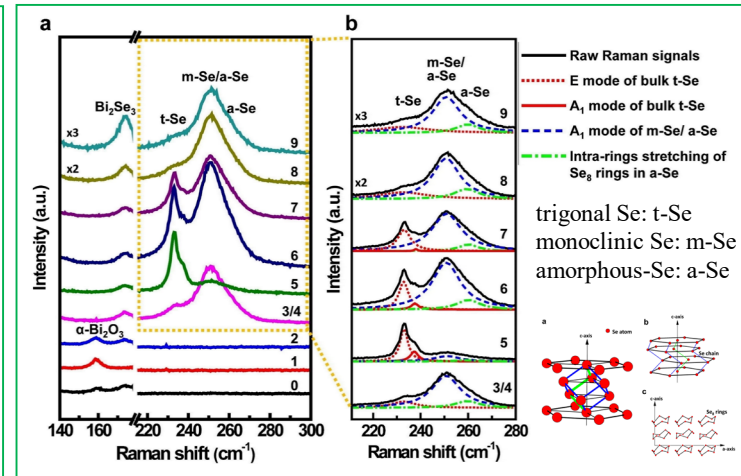
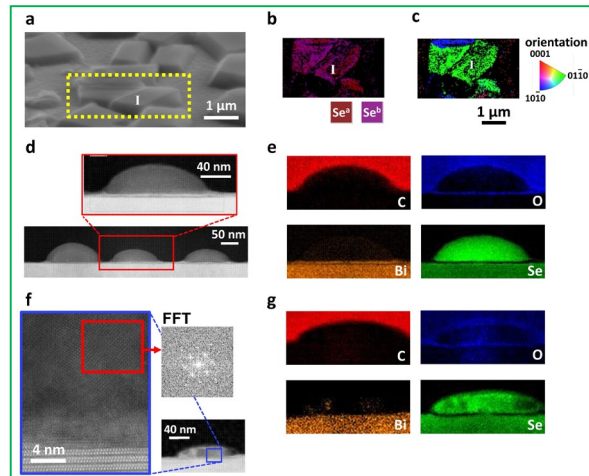
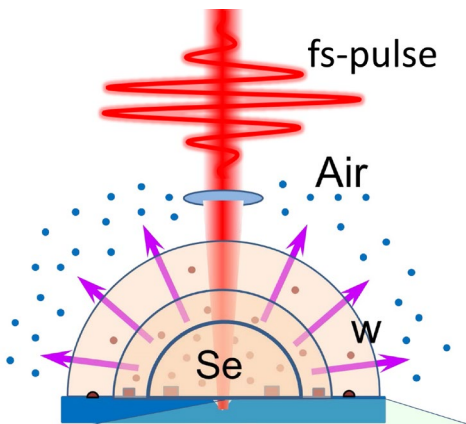
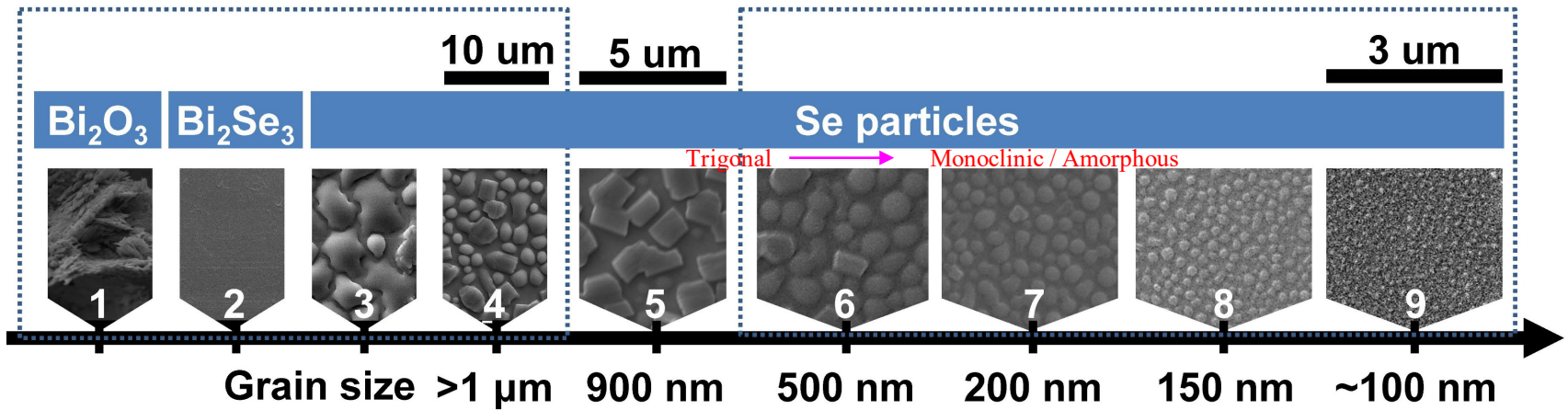


The size of ZnSe nanoparticles





Se nanoparticle prepared by fs Laser-induced plasma shock wave deposition





Outline

1. Introduction to femtosecond laser pulses
2. Nanoparticle fabrication
- 3. Nanostructure fabrication**
4. Ultrafast dynamics in topological insulators





Anisotropic optical transmission of femtosecond laser induced periodic surface nanostructures on indium-tin-oxide films

Chih Wang,¹ Hsuan-I Wang,² Chih-Wei Luo,^{2,a)} and Jihperng Leu^{1,b)}

¹*Department of Materials Science and Engineering, National Chiao Tung University, Hsinchu 300, Taiwan*

²*Department of Electrophysics, National Chiao Tung University, Hsinchu 300, Taiwan*

(Received 9 July 2012; accepted 27 August 2012; published online 7 September 2012)

Two types of periodic nanostructures, self-organized nanodots and nanolines, were fabricated on the surfaces of indium-tin-oxide (ITO) films using femtosecond laser pulse irradiation. Multiple periodicities (approximately 800 nm and 400 nm) were clearly observed on the ITO films with nanodot and nanoline structures and were identified using two-dimensional Fourier transformation patterns. Both nanostructures show the anisotropic transmission characteristics in the visible range, which are strongly correlated with the geometry and the metallic content of the laser induced nanostructures. © 2012 American Institute of Physics

Superior local conductivity in self-organized nanodots on indium-tin-oxide films induced by femtosecond laser pulses

Chih Wang,¹ Hsuan-I Wang,² Wei-Tsung Tang,² Chih-Wei Luo,^{2,4}
Takayoshi Kobayashi,^{2,3} and Jihperng Leu^{1,*}

¹*Department of Materials Science and Engineering, National Chiao Tung University, Hsinchu, Taiwan*

²*Department of Electrophysics, National Chiao Tung University, Hsinchu, Taiwan*

³*Department of Applied Physics and Chemistry and Institute for Laser Science, The University of Electro-Communications, Chofugaoka 1-5-1, Chofu, Tokyo 182-8585, Japan*

⁴cwluo@mail.nctu.edu.tw

^{*}jimleu@mail.nctu.edu.tw

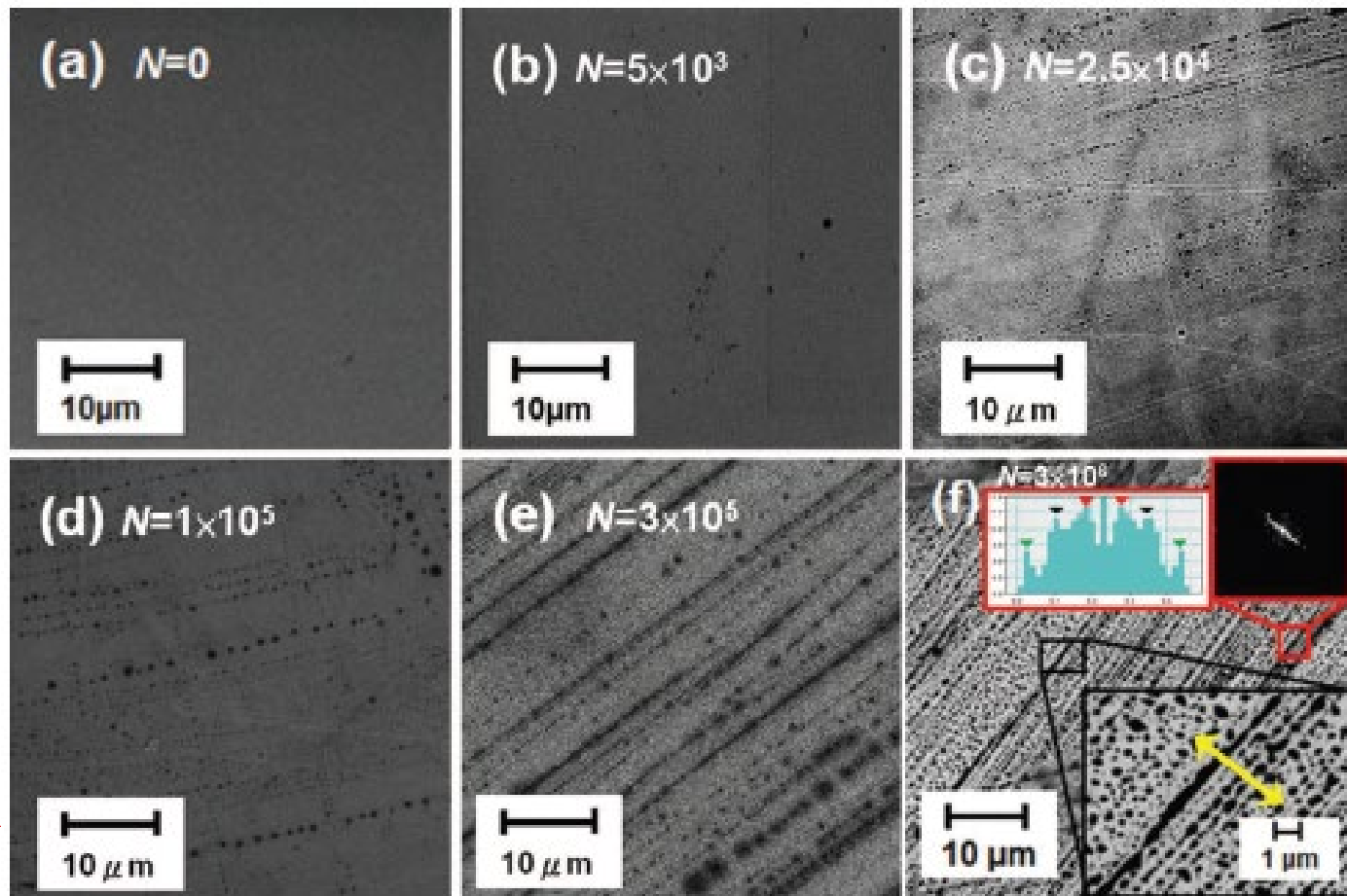
Received 31 Aug 2011; revised 23 Oct 2011; accepted 24 Oct 2011; published 14 Nov 2011

21 November 2011 / Vol. 19, No. 24 / OPTICS EXPRESS 24286



Nanostructure on ITO films

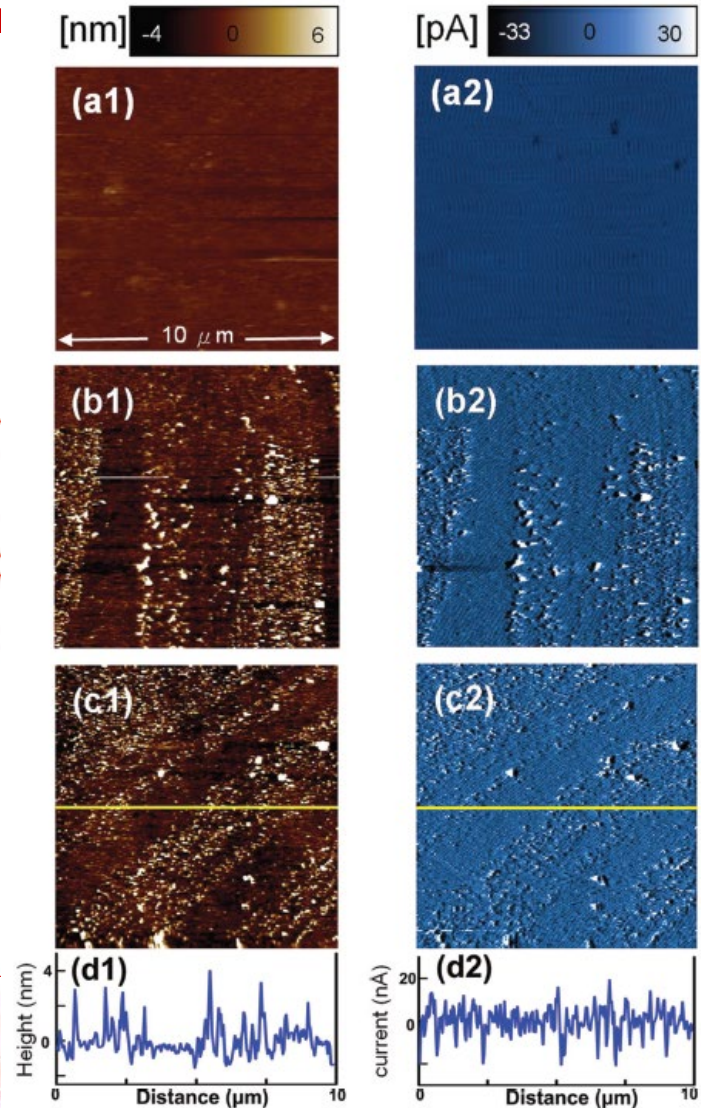
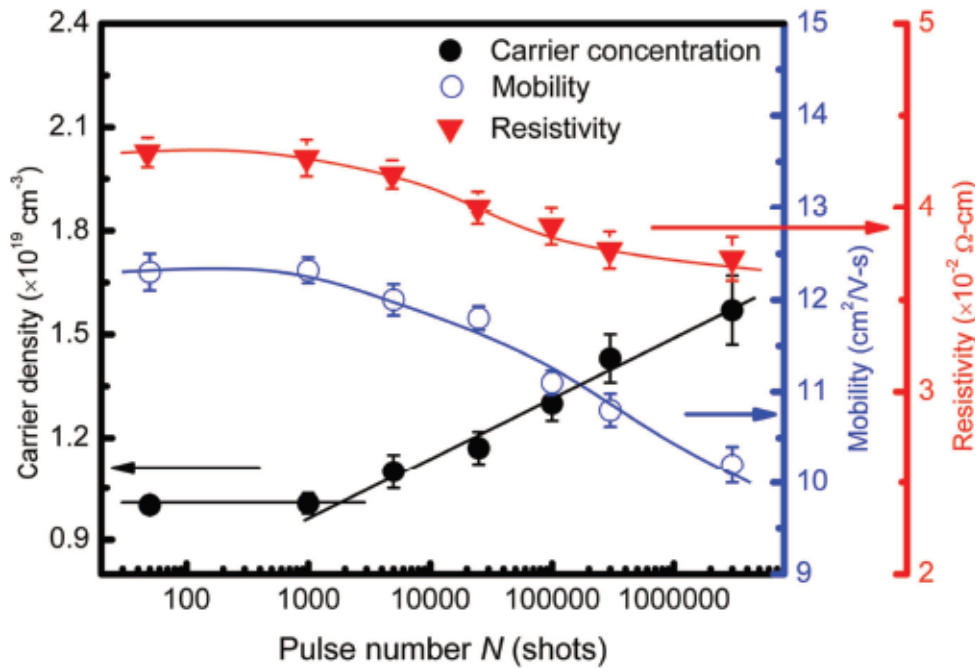
□ Pulse number-dependent nanostructure





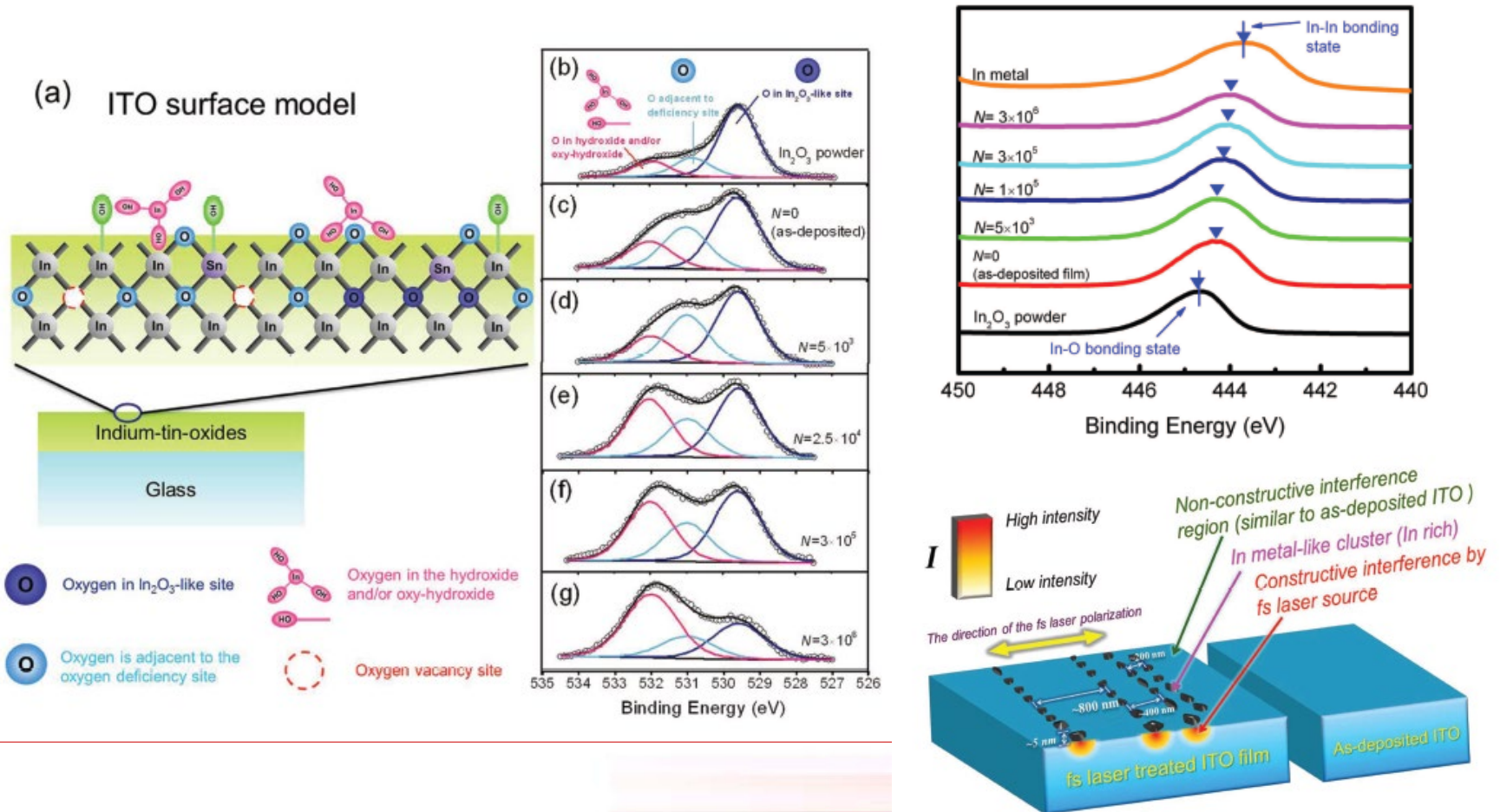
Nanostructure on ITO films

Transport properties



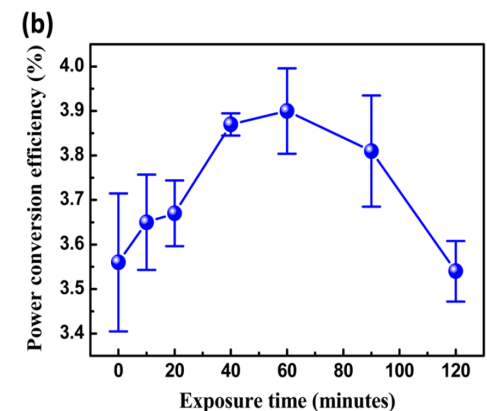
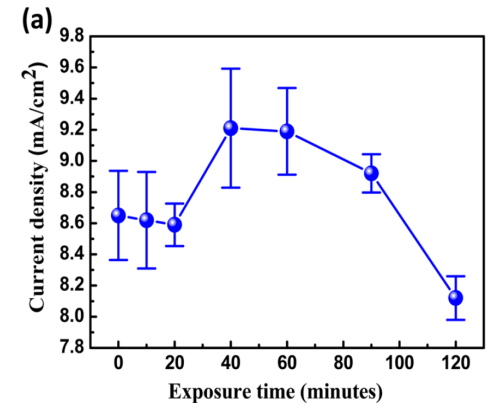
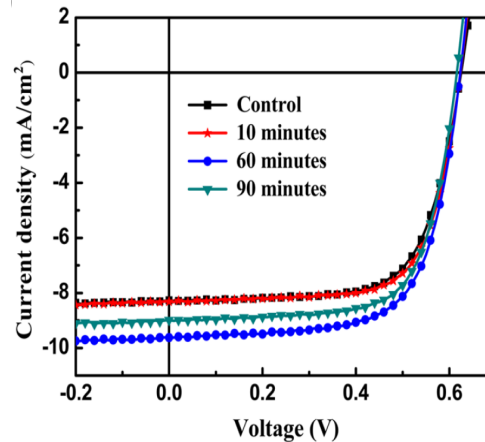
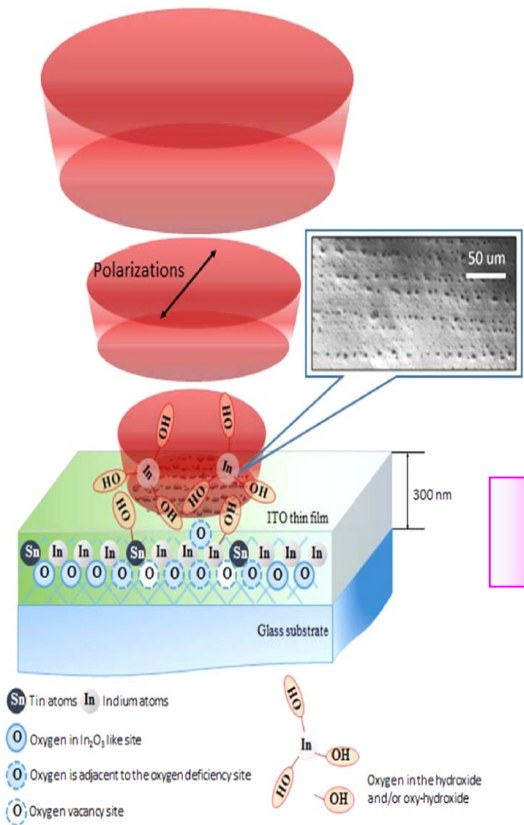
Nanostructure on ITO films

X-ray photoelectron spectroscopy (XPS)



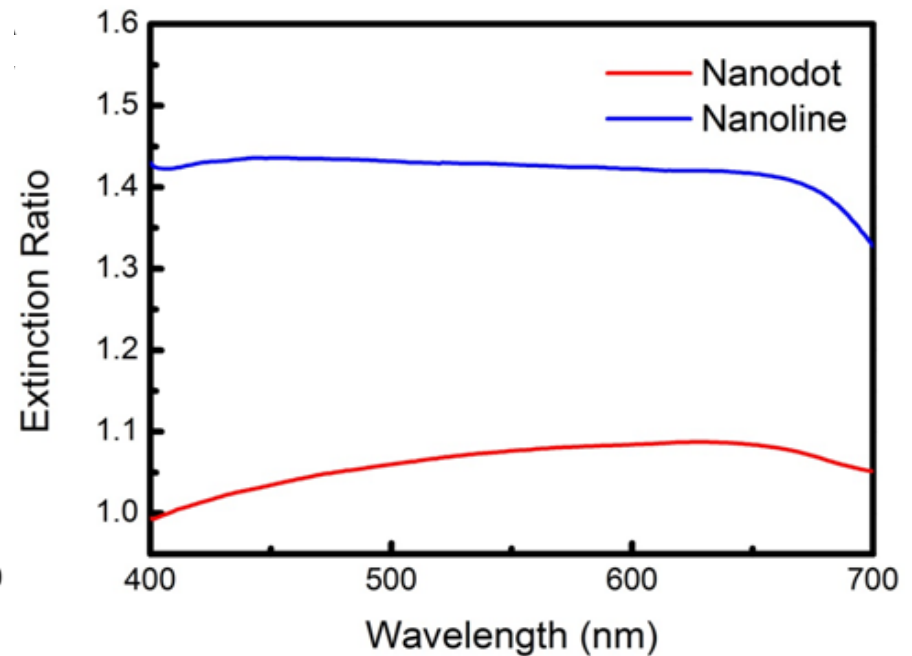
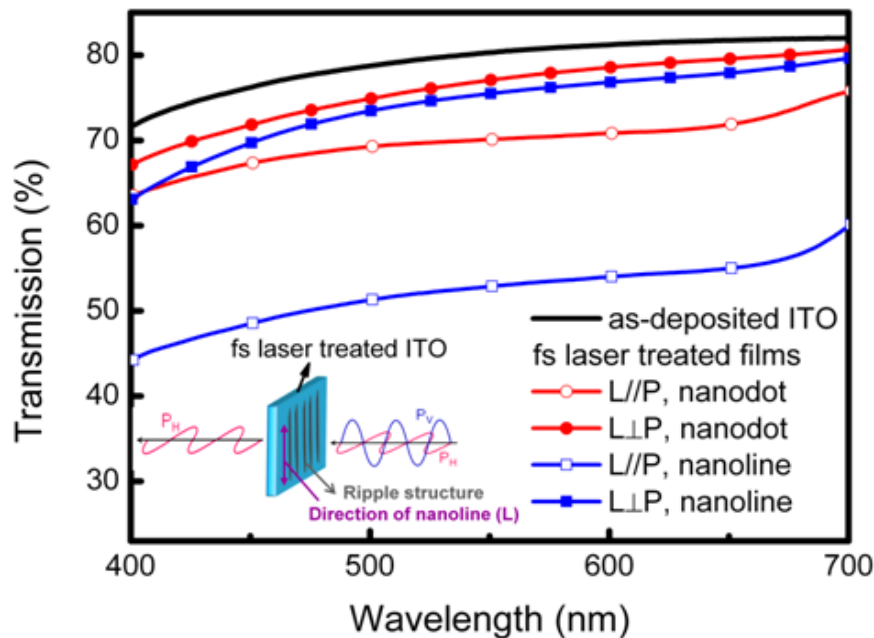
Application I

Effects on organic photovoltaics using fs-laser-treated ITO



Application II

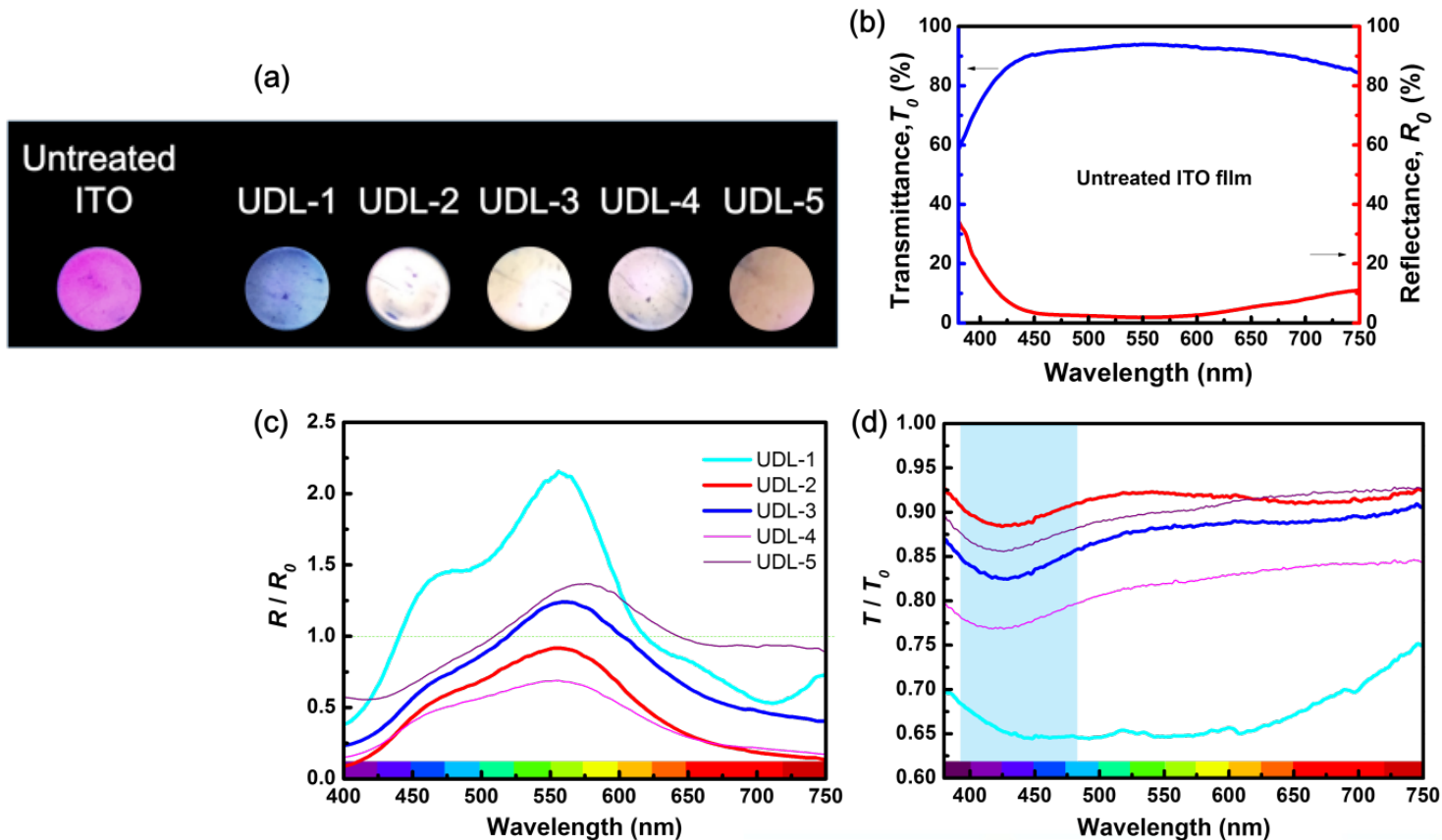
□ Anisotropic optical properties





Application III

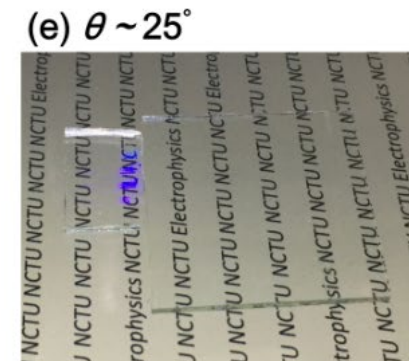
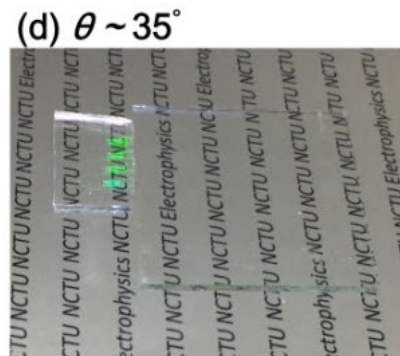
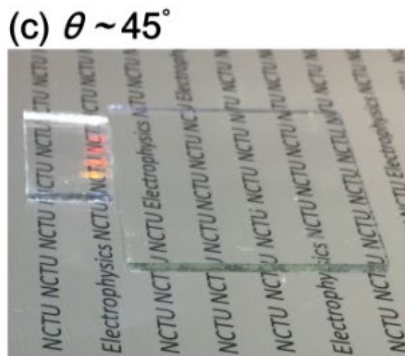
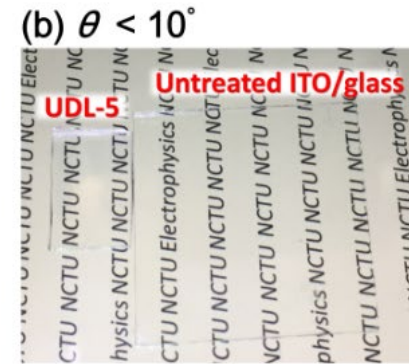
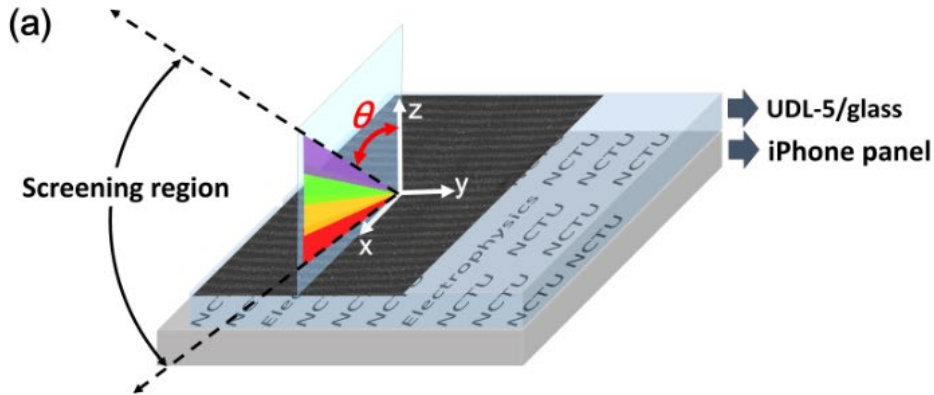
□ The colors of ITO films before and after laser processing.





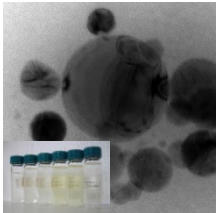
Application IV

- The image that is displayed on the LCD can be selectively screened by varying the view angle.

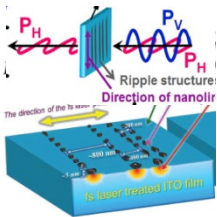




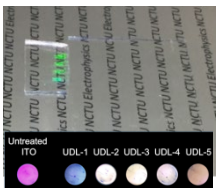
Summary I



- The hexagonal ZnSe & Se nanoparticles can be fabricated by properly controlling the fluences of the irradiating fs laser.



- The nanostructure with anisotropic transmission characteristics on ITO films induced by fs laser can be used for the alignment layer, polarizer and conducting layer in LCD cell.



- The nanostructure on the surface of ITO films significantly attenuates blue light, which are suited to eye protection and the screening of images behind ITO films for information security.



Outline

1. Introduction to femtosecond laser pulses
2. Nanoparticle fabrication
3. Nanostructure fabrication
4. Ultrafast dynamics in topological insulators





Platform for ultrafast dynamic study in Taiwan

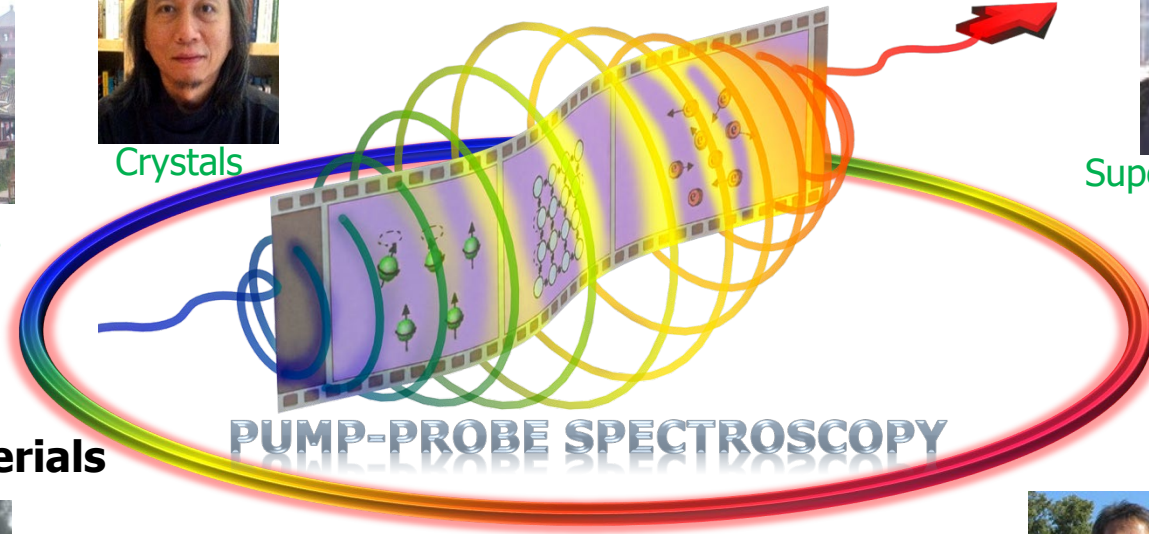
◆ Topological insulators



Thin films



Crystals



◆ Strongly correlated electron systems



Superconductors



Spin-glass systems

◆ 2D materials



Perovskite



2D transition metal dichalcogenide



Heterostructures
e.g., water splitting

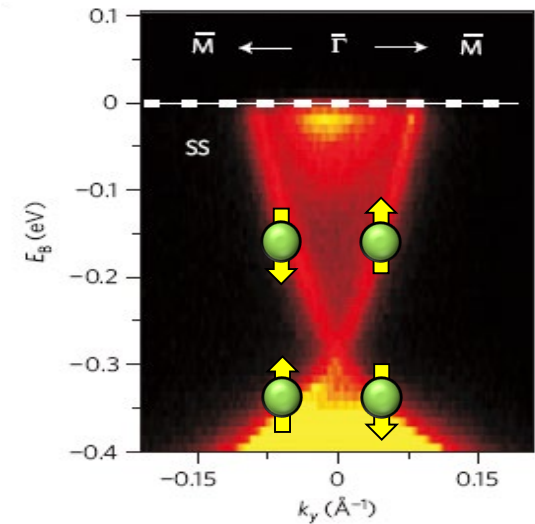
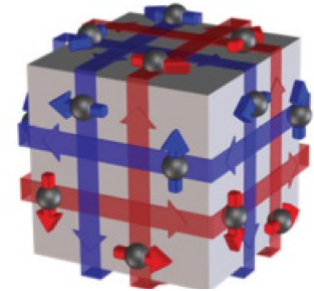
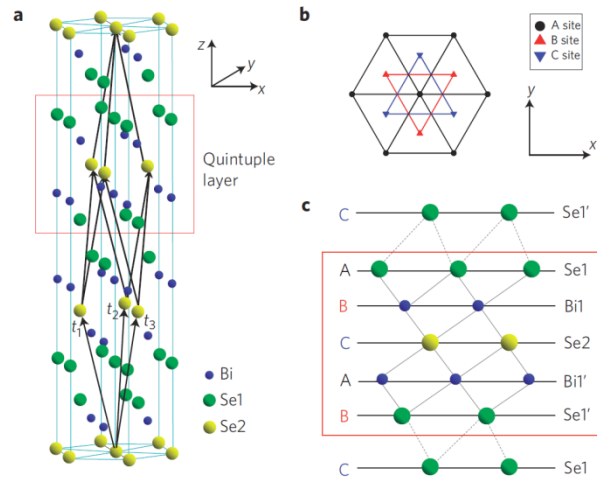
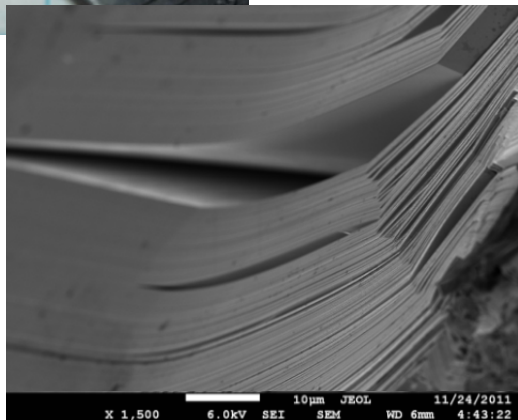
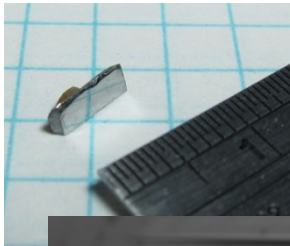


Intermetallics



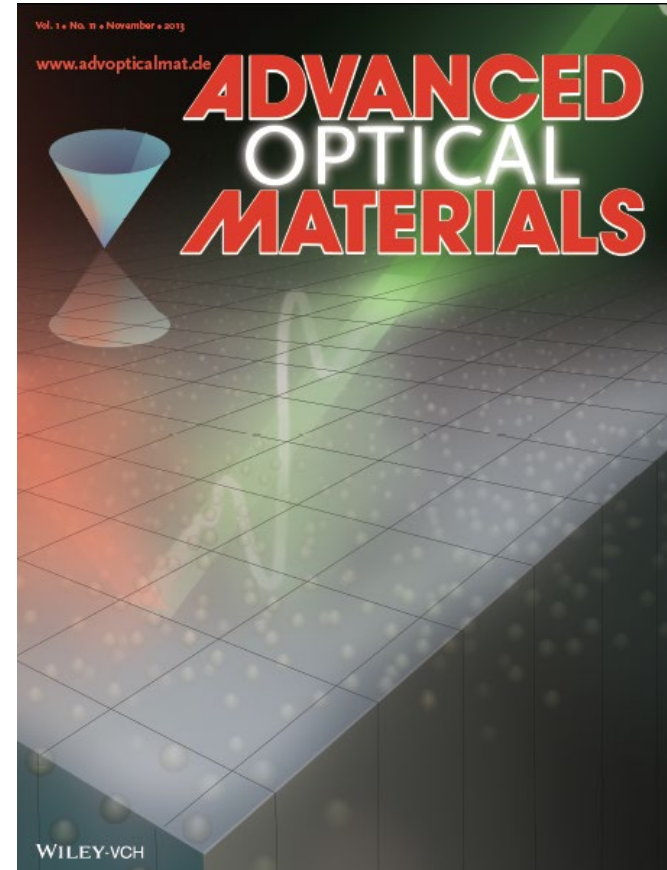
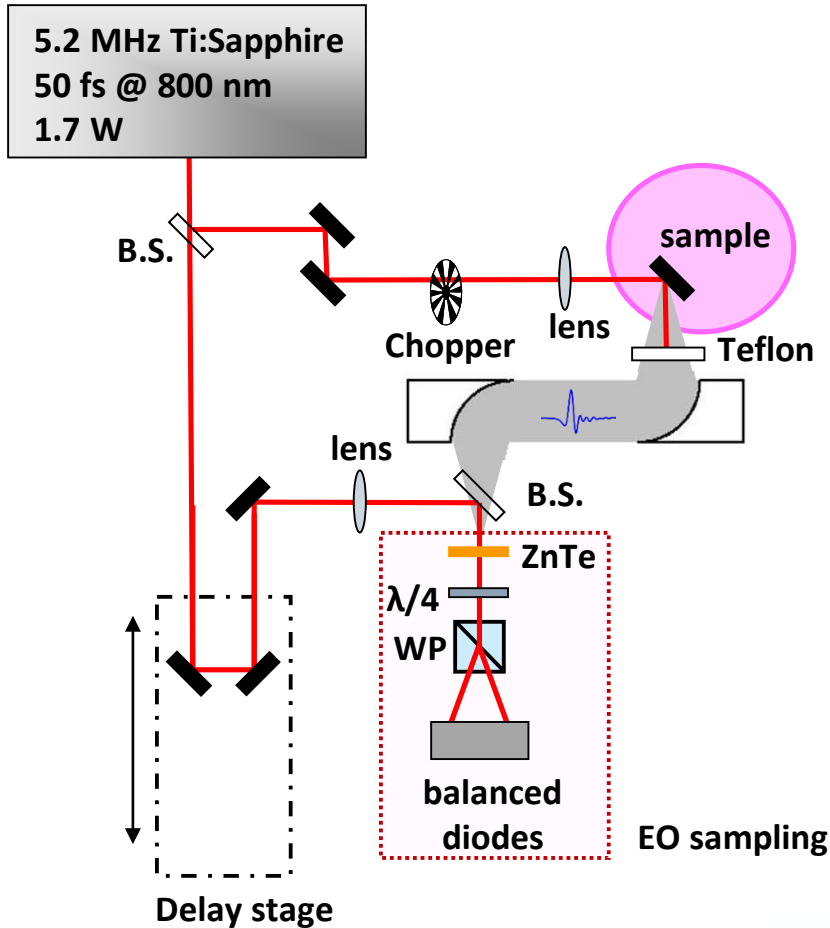
Topological insulators (TIs)

□ 3D TIs: Bi_2Se_3 , Bi_2Te_3 , ... etc.

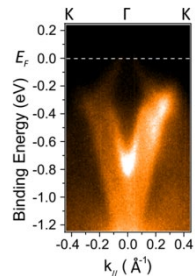




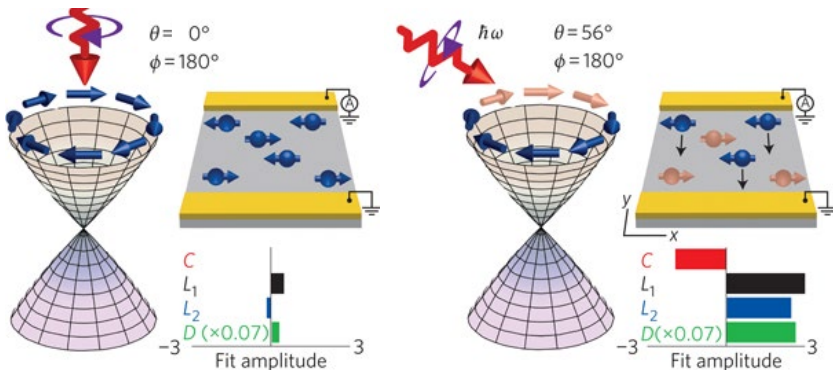
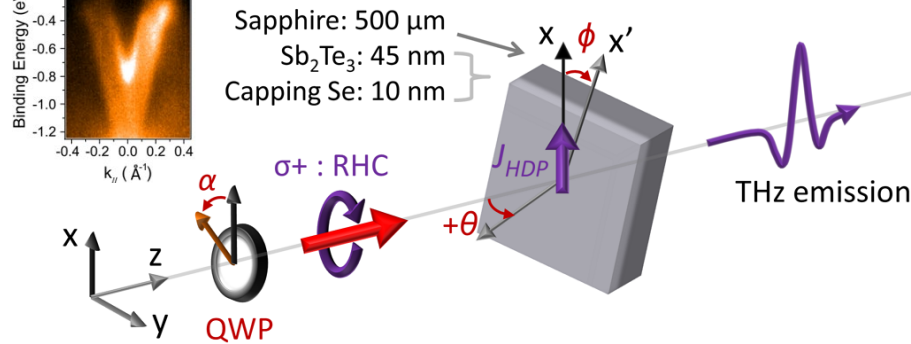
THz emission from topological insulators



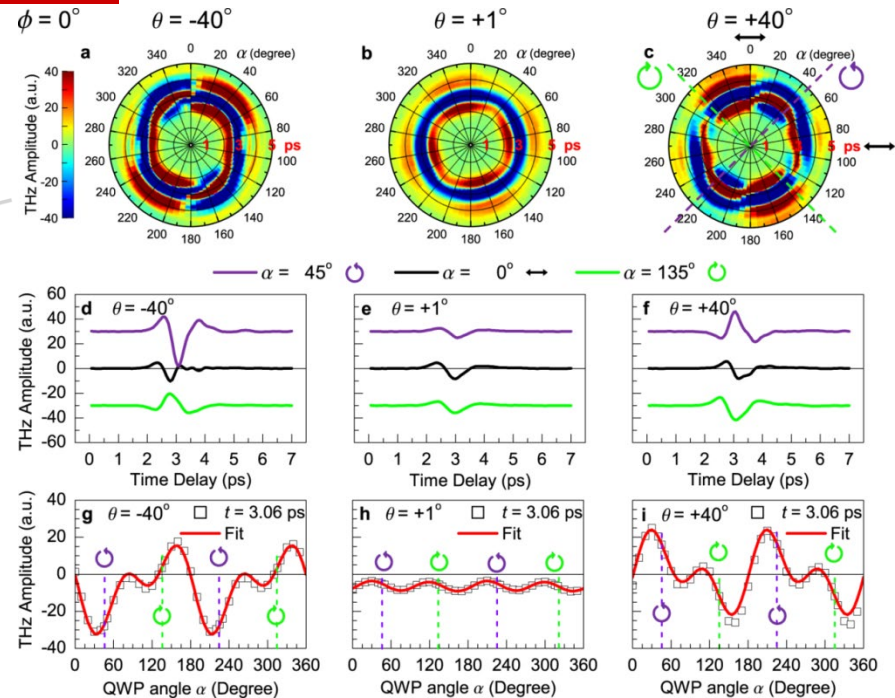
Mechanism of THz emission from TIs



Saphire: 500 μm
Sb₂Te₃: 45 nm
Capping Se: 10 nm



J. McIver et al, Nature Nanotech. **7**, 96 (2012).

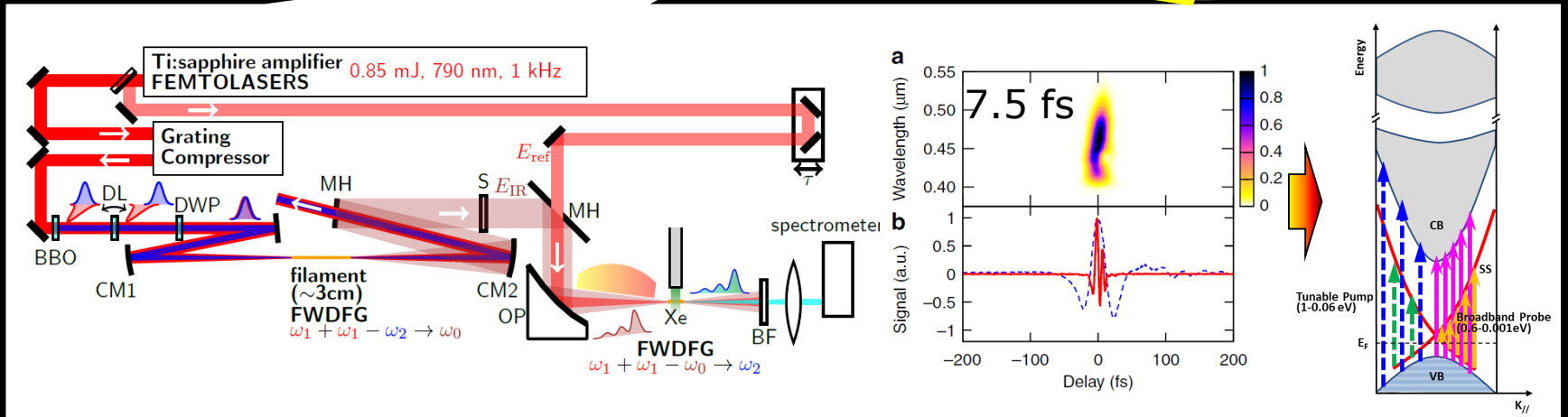
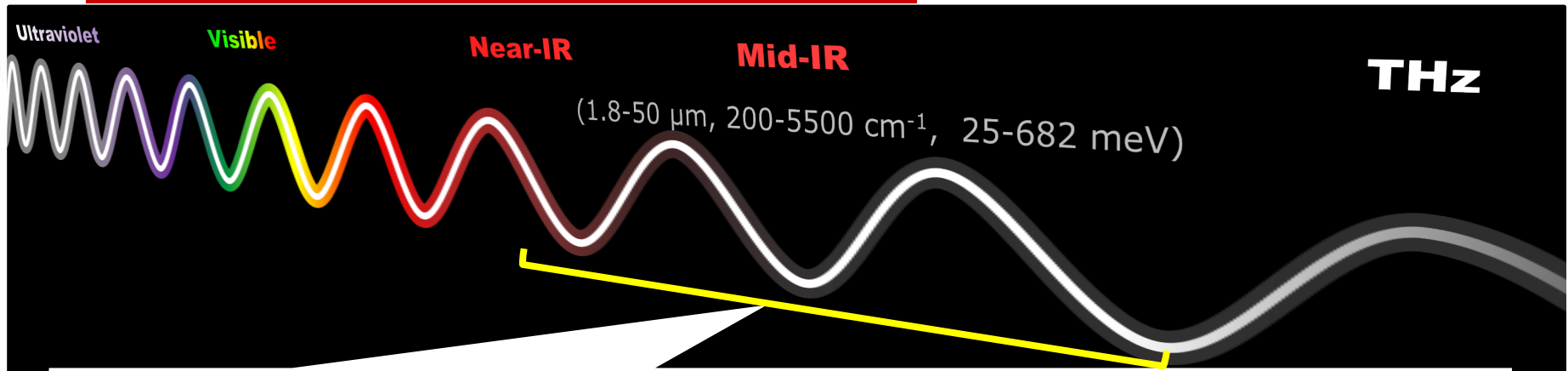


$$\vec{E}_{THz}(\alpha, t) \propto C'(t)\sin(2\alpha) + L'_1(t)\sin(4\alpha) + L'_2(t)\cos(4\alpha) + O(t)$$

- $C'(t)$: circular photogalvanic effect (CPGE) \rightarrow Surface state
- $L'_1(t)$: linear photogalvanic effect (LPGE) \rightarrow Surface state
- $L'_2(t)$: photon drag effect (PDE) \rightarrow Bulk state
- $O(t)$: optical rectification (OR) \rightarrow Bulk state

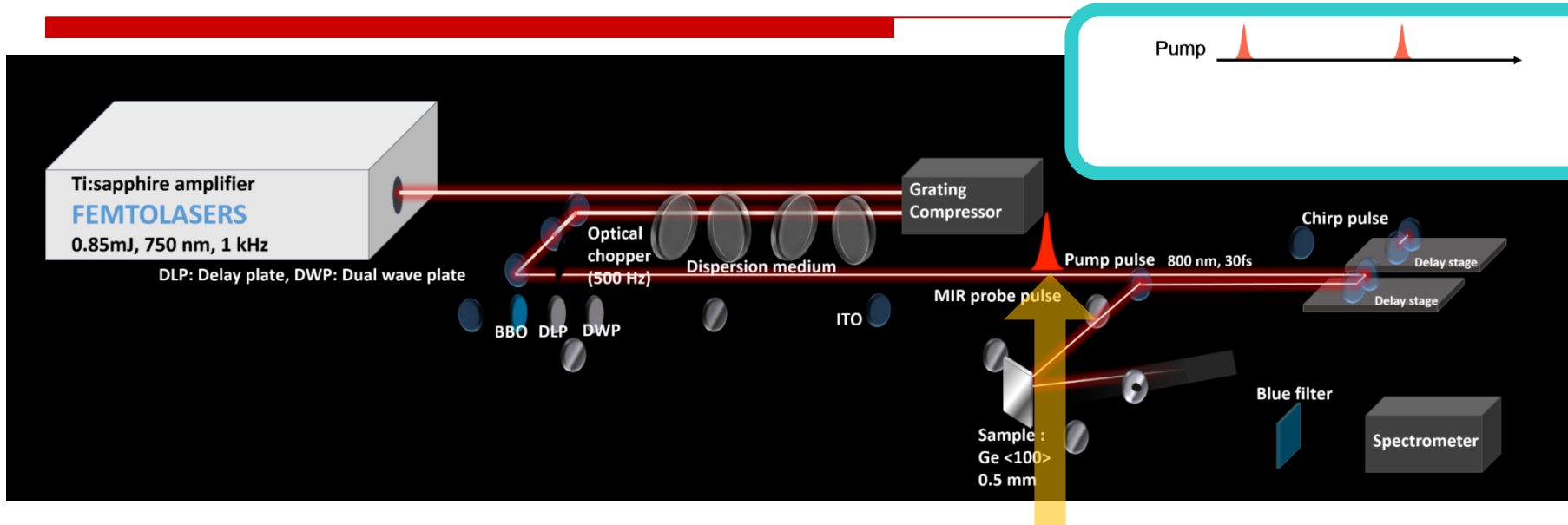


Ultrashort-pulse light sources in UDL





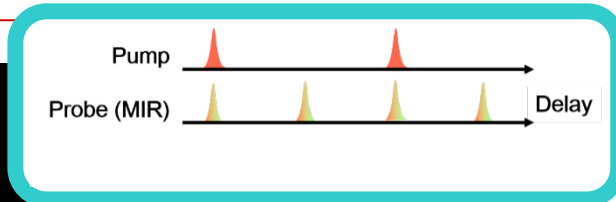
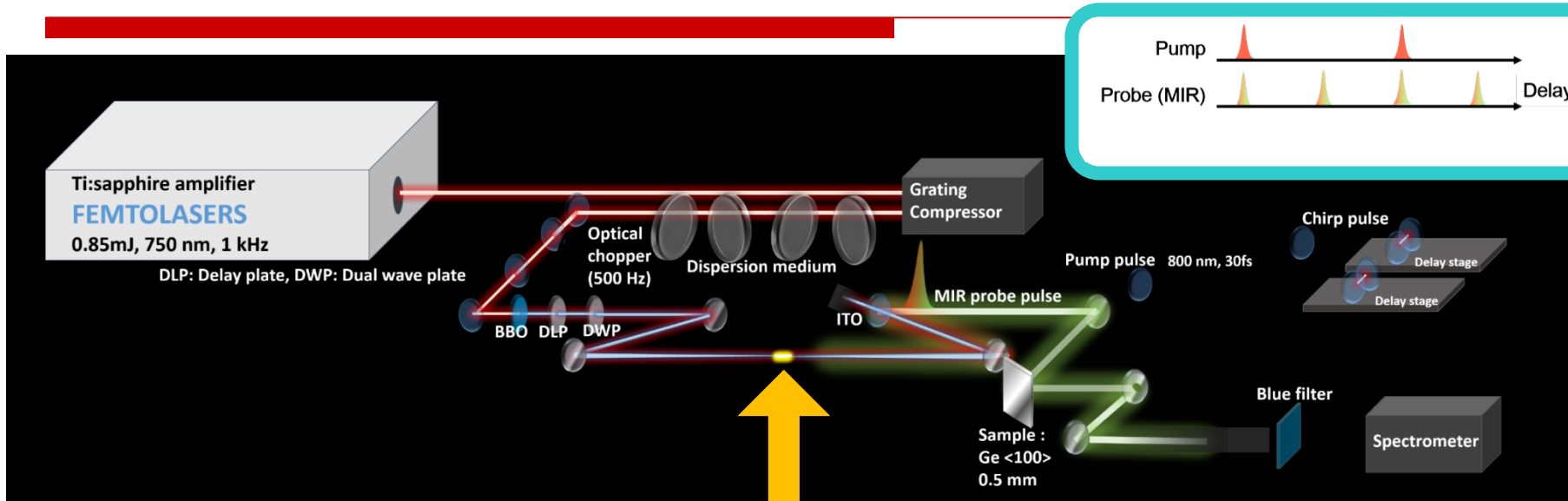
800 nm pump & ultrabroadband mid-IR probe



Pump beam : 800 nm (1.55 eV), 30fs



800 nm pump & ultrabroadband mid-IR probe



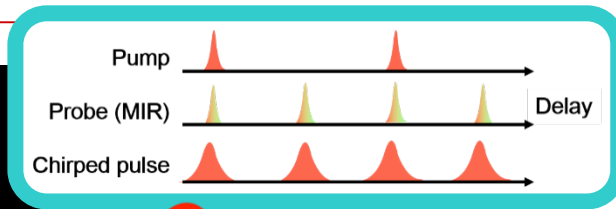
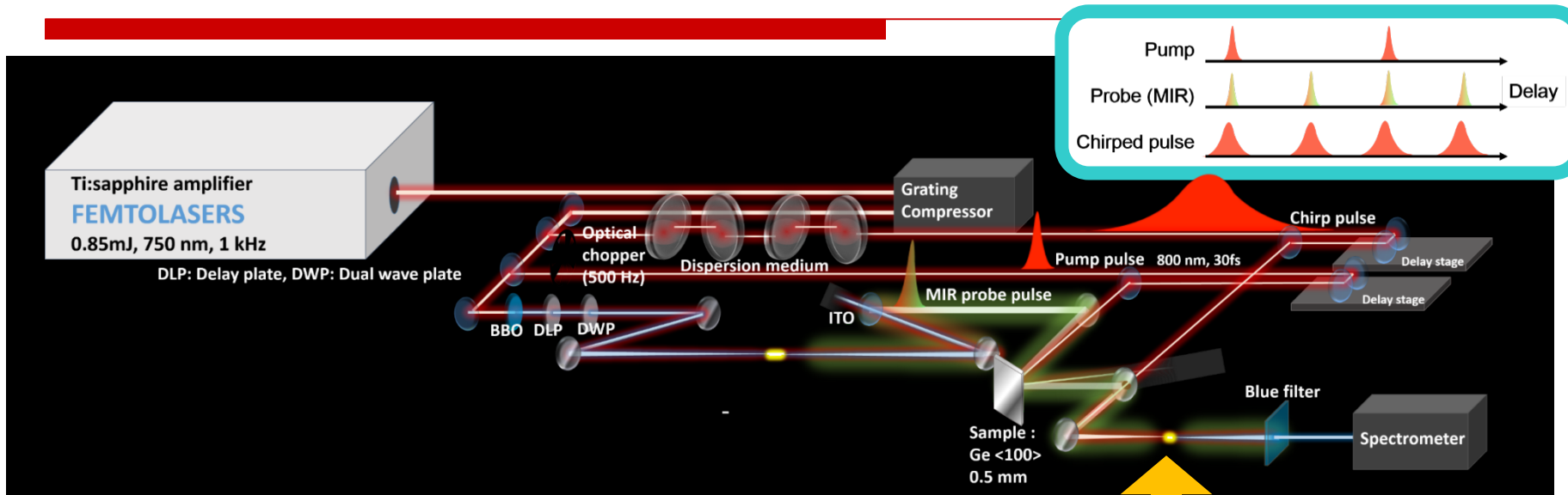
Probe beam : Mid-infrared
 Four-wave difference frequency generation (FWDFG)

Pulse width: 7 fs
 Band width: 200-5000 cm⁻¹

$\omega_1 + \omega_1 - \omega_2 \rightarrow \omega_3$
 800nm + 800nm - 400nm = MIR



800 nm pump & ultrabroadband mid-IR probe



Detection: Upconversion (FWDFG)

- Broadband capability
- High sensitivity
- High speed scan

Reference pulse ω_1

Air ω_4

Spectrometer

Sample ω_3

$\omega_1 + \omega_1 - \omega_3 \rightarrow \omega_4$

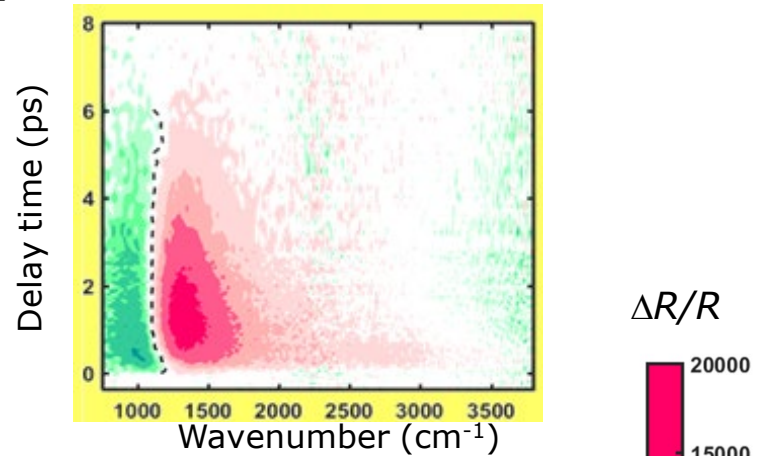
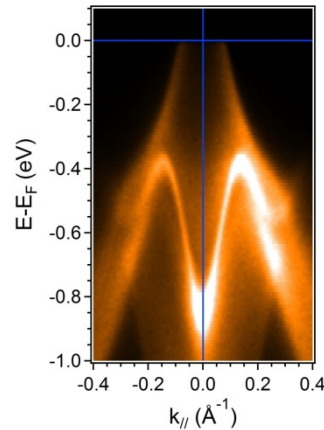
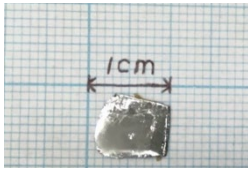
800nm 800nm MIR $\sim 400\text{nm}$



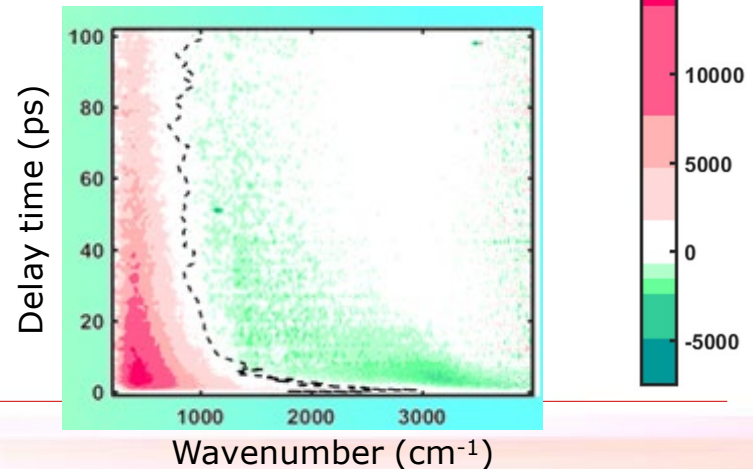
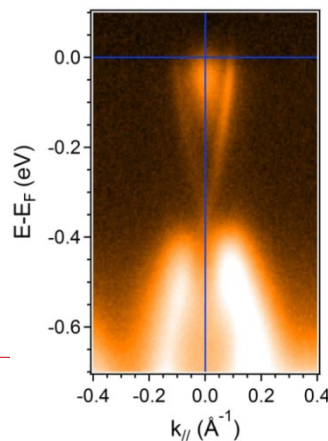
Ultrafast dynamics in topological insulators

□ $\text{Sb}_2\text{Te}_2\text{Se}$ single crystals (p-type)

Pump beam fluence : 101 ($\mu\text{J}/\text{cm}^2$)



□ $\text{Bi}_2\text{Te}_2\text{Se}$ single crystals (n-type)





The sign changes of $\Delta R/R$

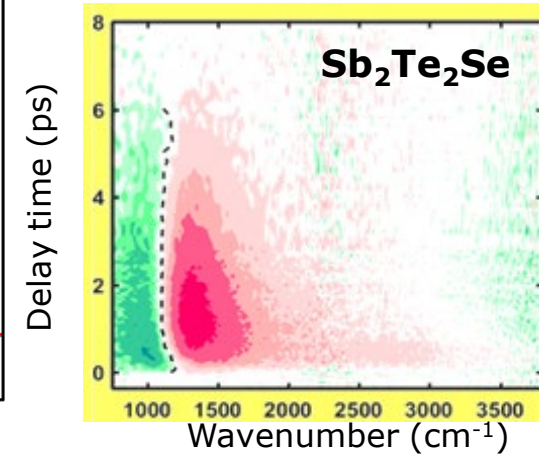
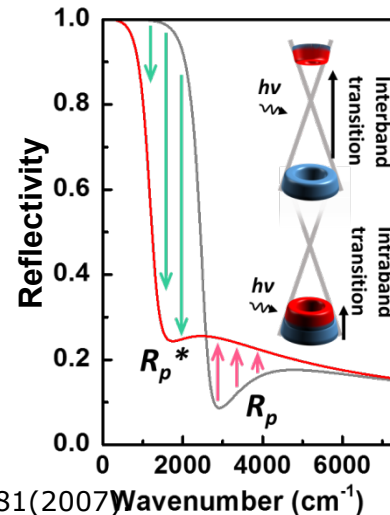
Surface carrier transition

$$\varepsilon(\omega) = \frac{-8T}{\omega(\omega + i\tau^{-1})} \ln \left[2 \cosh \left(\frac{E}{2T} \right) \right] + \frac{\pi i}{\omega} \left[G \left(\frac{\omega}{2} \right) - \frac{4\omega}{i\pi} \int_0^{+\infty} d\varepsilon \frac{G(\omega) - G \left(\frac{\omega}{2} \right)}{\omega^2 - 4\varepsilon^2} \right]$$

E : energy level, T : temperature

Falkovsky model

L. A. Falkovsky, and A. A. Varlamov, A. Eur. Phys. J. B. **56**, 281(2007)

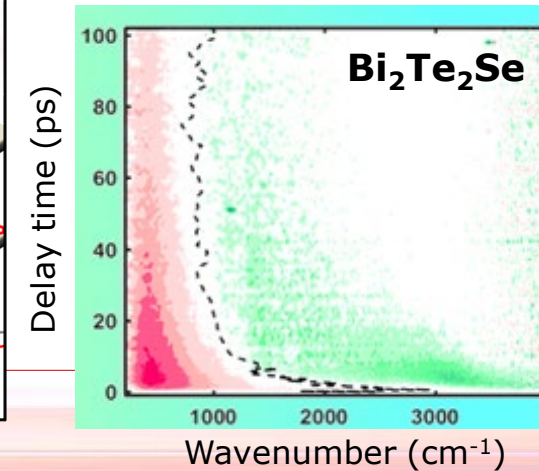
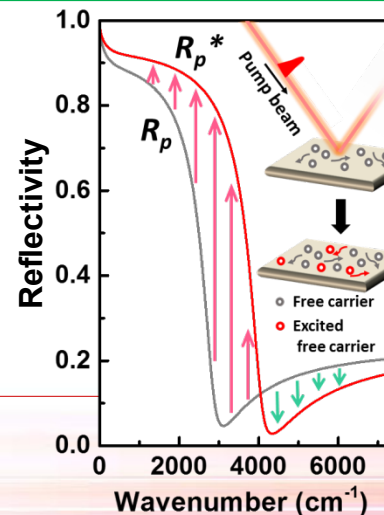


Free carrier absorption

Drude model $\varepsilon(\omega) = \varepsilon_{\infty} - \frac{\omega_p^2}{\omega^2 + i\Gamma\omega}$

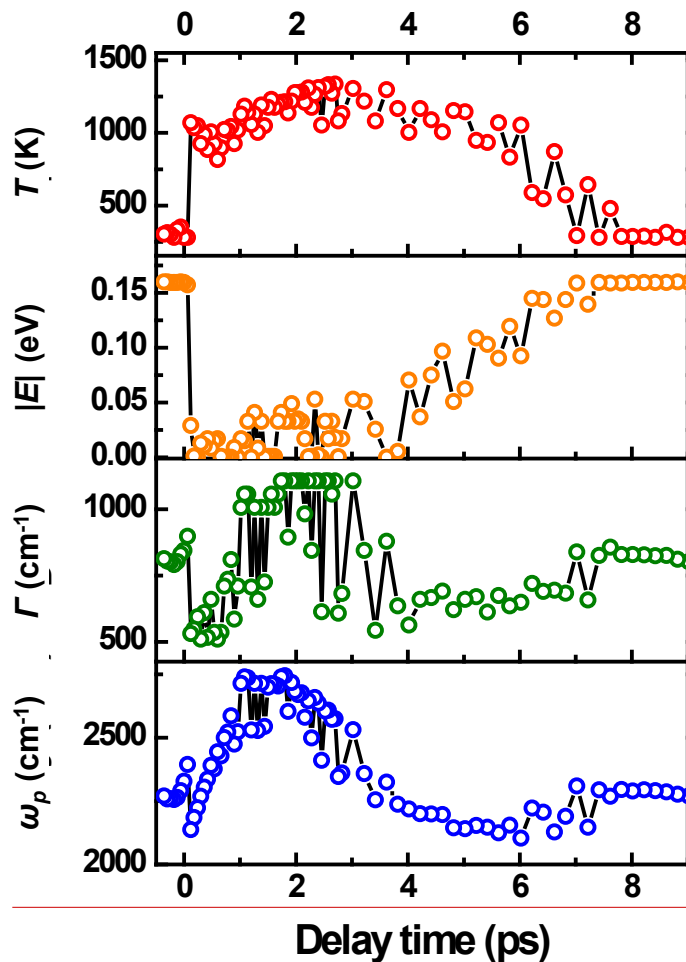
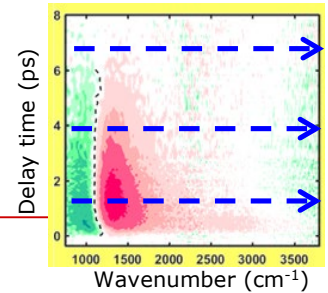
ω_p : plasma freq.
 Γ : scattering rate

Carrier concentration: $N = \frac{m^*}{4\pi e^2} \omega_p^2$

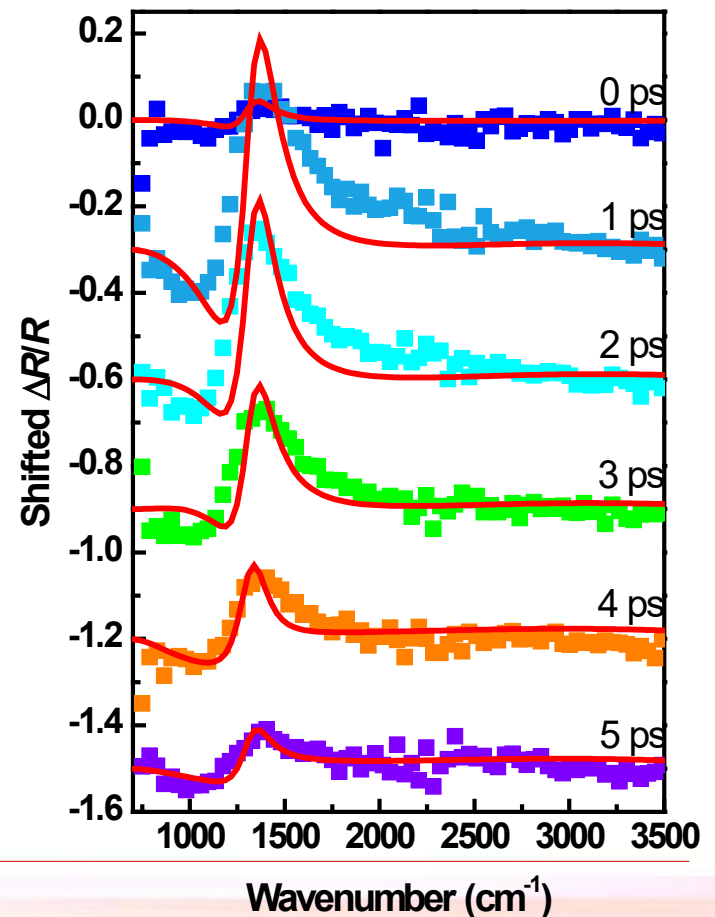
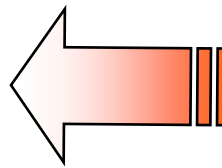




Relaxation processes in $\text{Sb}_2\text{Te}_2\text{Se}$

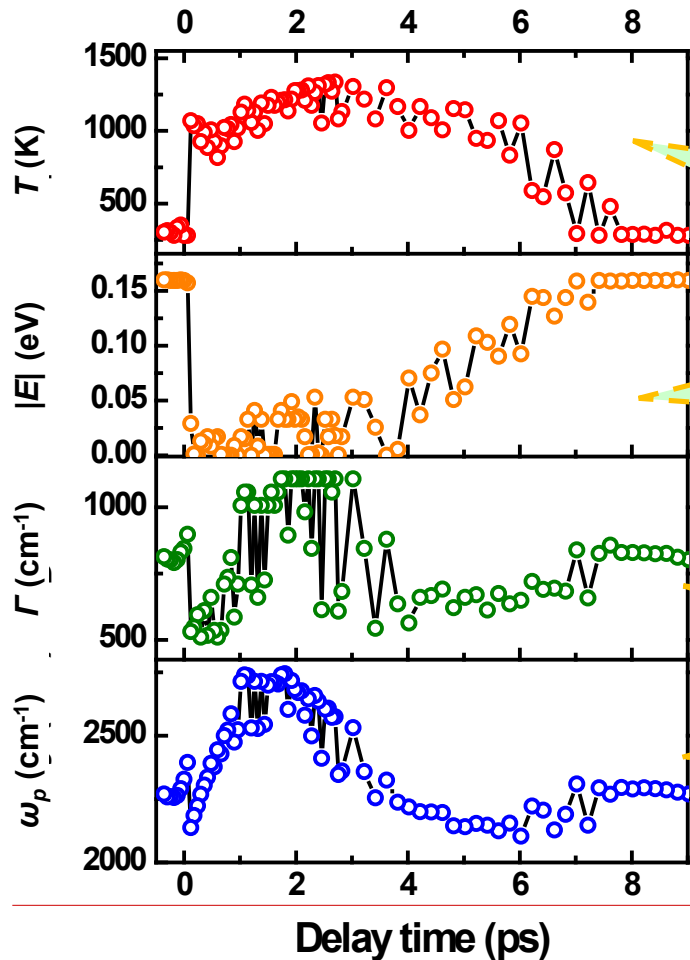


Fitted by Falkovsky model

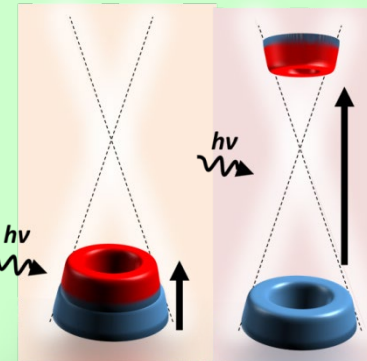




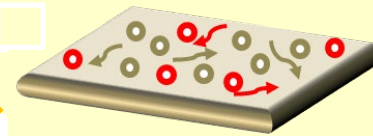
Relaxation processes in $\text{Sb}_2\text{Te}_2\text{Se}$



Surface carrier transition

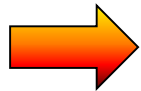
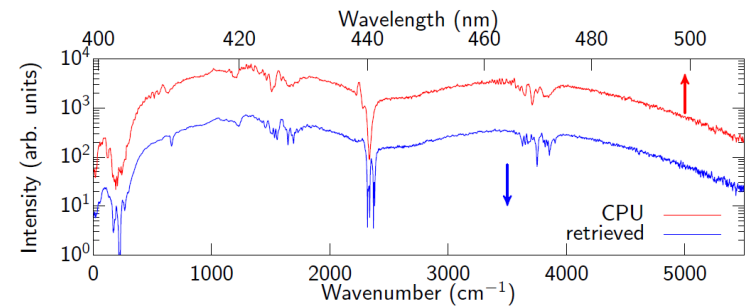
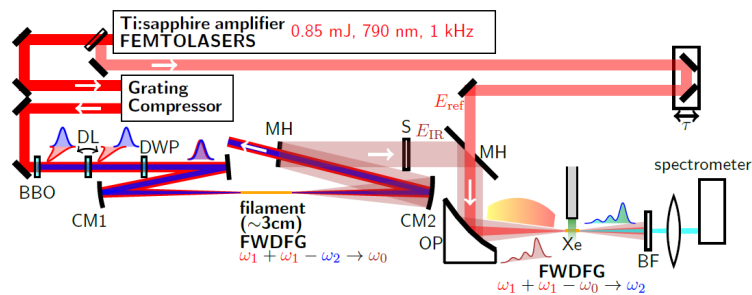


Free carriers



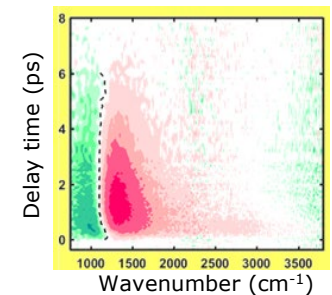
Summary II

◆ Ultrabroadband mid-IR generation & detection



Time-resolved + FTIR

- ◆ Reveal the full ultrafast dynamics in topological insulators.
- ◆ Apply to study the vibration dynamics of molecules in femtosecond timescale.



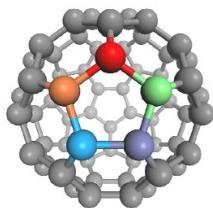


國立交通大學

National Chiao Tung University

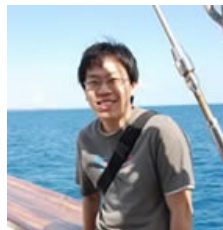
Acknowledgements

科技部



TCECM

Group members





國立交通大學

National Chiao Tung University

*Thank you
for your attention!!*



NCTU Museum

